Late Holocene earthquakes at the Mudurnu valley, 1967 earthquake segment of the North Anatolian Fault Zone, recorded in river channel deposits

NIKOLAOS PALYVOS[1], DANIELA PANTOSTI[1], CENGIZ ZABCI[2], GIULIANA D'ADDEZIO[1]

1: Istituto Nazionale di Geofisica e Vulcanologia (Rome), Italy.

2: Istanbul Technical University (ITU), Turkey

Corresponding author addresses:

N. Palyvos, INGV (Roma), Sezione di Sismologia e Tettonofisica, Via di Vigna murata 605, 00143 Roma, Italia. e-mail: palyvos@ingv.it, tel: +39 06 51860545

Abstract

This study provides constraints on the recurrence of recent surface-rupturing earthquakes at the southern (main) branch of the North Anatolian Fault Zone (Turkey), west of the Bolu basin. The target was the fault segment that ruptured during the 1967 Mudurnu valley earthquake (Ms 7.1), which preceded the devastating earthquakes of 1999 in the sequence of westward-migrating earthquakes since 1939.

A trench was excavated on a Late Holocene terrace in the fault-line valley of the Mudurnu River, across a low fault scarp that was followed by the 1967 surface rupture. Three fault zones were exposed in river channel deposits: two recently active ones, bounding a subtle pressure ridge (push-up) superimposed on the scarp, and a sealed one in-between them. Detailed logging of the stratigraphy revealed a minimum of three (possibly four) paleoearthquakes, preceding the 1967 earthquake.

The most conservative interpretation of maximum-limiting radiocarbon ages, is that the youngest 2 (possibly 3) paleoearthquakes have occurred since AD1394 (max. average recurrence interval 286 yrs / possibly 191 yrs), whereas the older event is unconstrained. A second interpretation that is not to be excluded based on the inconclusive historical earthquake record, suggests that all three (possibly four) paleoearthquakes recognised in the trench, may have occurred since ca. AD1668 (max. average recurrence interval 100 yrs / possibly 75 yrs).

Keywords: Earthquake Geology, Paleoseismology, strike-slip fault, Pressure ridge, North Anatolian Fault Zone.

Introduction – Aim of study

The dextral strike-slip North Anatolian fault zone (NAFZ – Fig. 1) is a major, active, and highly seismogenic structure in the Eastern Mediterranean, spanning more than 1500 km from eastern Turkey to the North Aegean Sea and the coast of mainland Greece. It accommodates the westward extrusion of the Anatolian (Asia Minor) micro-plate, which is caused by the Arabia-Eurasia collision (e.g. McKenzie 1972; Ambraseys 1970; Şengör 1979; Barka 1992; Bozkurt 2001; Şengör et al. 2004). The present-day westward velocity of Anatolia relative to Eurasia is of the order of 22±3 mm/yr (Straub et al. 1997), and their relative motion is largely accommodated by the NAFZ.

Whereas the NAFZ consists of one main active branch at its central part, it becomes progressively more complex to the W of the Bolu basin (Figs. 1 and 2a), where a first major bifurcation occurs. In this area, the southern branch follows the Mudurnu River valley (Fig. 2) and is considered as the main structure (e.g. Barka 1992; Neugebauer et al. 1997). It hosted the Mudurnu valley (1967) and Abant (1957) earthquakes (e.g. Ambraseys and Zatopek 1969, Barka, 1996) that preceded the devastating earthquakes of August and November 1999 at the western part of the NAFZ (Figs 1 and 2a - e.g. Barka et al. 2002; Akyüz et al. 2002). These recent earthquakes extended farther W the portion of the NAFZ that has ruptured since 1939, in a quasi-systematic pattern of westward-migrating, successive large earthquakes (e.g. Ambraseys 1970; Barka, 1996; Stein et al. 1997), leaving a seismic gap in the Marmara sea area and heightened earthquake hazard threatening the city of Istanbul (e.g. Atakan et al. 2002).

Knowledge of the spatial and temporal complexity of earthquake recurrence along large, segmented seismogenic fault zones such as the NAFZ, is essential to an eventual understanding of the behaviour of these fault zones and to reliable earthquake hazard evaluations and forecasts (Sieh 1996). The aim of this study was to obtain information on

earthquake recurrence at the Mudurnu valley branch of the NAFZ (Fig. 2a) and in specific, the earthquake segment of July 22, 1967 (Fig. 2b - Ambraseys and Zatopek 1969). With respect to earthquake recurrence, this is one of the least studied segments of the NAFZ in the area of Fig. 2a. Aerial photograph analysis and geomorphological field reconnaissance were carried out to select a suitable site on the 1967 rupture, where we excavated a reconnaissance trench for paleoseismological analysis (e.g. Sieh 1978; McCalpin 1996; Yeats et al. 1997).

The Mudurnu valley, July 22, 1967 earthquake segment and state of knowledge of its seismic history

The Mudurnu valley earthquake of 22 July 1967 was a large (Ms 7.1), complex event (e.g. Pinar et al. 1996), that caused substantial damage (Ambraseys and Zatopek 1969) and may have brought closer to failure the August 1999 earthquake segment of the NAFZ (e.g. Muller et al. 2003). Ambraseys and Zatopek (1969) meticulously mapped ca. 55 km of continuous surface rupture (Fig. 2b), that probably switched to distributed deformation for an additional 25 km towards the W (up to lake Sapanca – Fig. 2a). The easternmost 25 km of the 1967 surface ruptures overlapped (or coincided with) the ruptures of the previous large earthquake at this part of the zone, the Ms 7.0 Abant earthquake of 1957 (Fig. 2a), at an area proposed to be a potential seismic barrier (Michel and Janssen 1996).

Ambraseys and Zatopek (1969) reported maximum relative displacements of 190 cm lateral and 120 cm vertical, but also noted that the far-field horizontal displacement may have been substantially larger than these measurements, that were made along discrete surface breaks. According to the same authors, the coseismic deformation was distributed

in a zone ranging from a few meters up to 2-3 km in width, reflecting the structural complexity of the NAFZ at a close scale (see Michel et al. 1995 for our trench area, or Neugebauer 1995 and Michel and Janssen 1996, for the E part of the valley).

Although a large number of earthquakes in the broader region of Fig. 2a is recorded in historical accounts (e.g. Ambraseys and Finkel 1995; Ambraseys and Jackson 1998; Ambraseys 2002; Guidoboni et al. 2004), the available information so far does not really allow a safe correlation of any of them to rupture of the branch of the NAFZ passing through the Mudurnu valley, which is a rather secluded place without any large population centre (the town of Mudurnu is actually to the S of the valley, Fig. 2a). In most cases, candidate faults can be more than one. According to a revision of historical earthquake catalogues until AD1500 by Guidoboni et al. (2004), several historical earthquakes were strongly felt in the broader area that encompasses the cities of Iznik (Nicaea), Izmit (Nicomedia), Mudurnu (Mouthoupolis), the Duzce plain and Bolu (Claudiopolis) – Fig. 2a. These earthquakes occurred in AD 29 (or 32), 69, 120, 181, 268, 358, 362, 368, 447, 554, 740?, 967, 1065. Macroseismic epicentre determinations by Guidoboni et al. (2004) are only very roughly indicative of possible epicentral regions. Among the earthquakes mentioned above, the epicentre that appears closest to the Mudurnu valley is that of AD 181. Ambraseys and Jackson (1998) report also a probable earthquake affecting the Mudurnu area in 1419. Of the earthquakes in the period AD 1500-1800 discussed in Ambraseys and Finkel (1995), those that involved damage at areas close to the Mudurnu valley are those of 1668, 1719 and 1754. The great 1509 Marmara earthquake caused severe damage up to at least Bolu (Ambraseys and Finkel 1995), thus it can also be included in the list (Langridge et al., 2002, include the Mudurnu valley in the possible earthquake segment). Large earthquakes in the past (like 1509 or 1668) may have been multiple events involving very long stretches of the NAFZ. E.g., the surface rupture of the Erzincan, 1939, Ms 7.8 earthquake was about 350 km (Barka 1996 and references therein).

A revised catalogue for AD1500 to present by Ambraseys (2004) includes historical epicentres at the Sapanca lake area in AD 1567, 1878 and 1894.

Paleoseismological studies on the Mudurnu valley branch of the NAFZ have been conducted by Ikeda et al. (1991) at the central part of the 1967 rupture and, Demirtas (1996, 2000) at the overlap area between the 1967 and 1957 ruptures. In the latter area trenches were also excavated by Michel and Janssen (1996), but were oriented more towards structural analysis. Ikeda et al. (1991) constrained the penultimate event (the one preceding that of 1967) to be for sure after AD 1480 and, they further proposed that it may have been the large earthquake of 1668. Demirtaş (1996) recognised a possible cluster of earthquakes around 4335-3995 BC but, did not obtain information about the earthquake history of the fault zone in more recent times.

Trench site selection and geomorphology

We ruled out of our investigation the eastern part of the 1967 rupture that overlapped with the 1957 rupture (Fig. 2b), in order to avoid obtaining a record of overlapping ruptures, as well as the western one, where the fault splays in several strands in a zone of diffuse deformation and folding (Ikeda et al. 1989, 1991). With the map of the 1967 ruptures by Ambraseys and Zatopek (1969) as a guide, we focused at locating areas favourable for trenching at the central part of the rupture, using aerial photo interpretation and geomorphological reconnaissance in the field. Finding a promising trench site in this area proved to be difficult, due to: (a) stretches of the rupture being along slopes where landsliding occurs / has occurred, (b) dense vegetation and cultivations, and (c) man-made modification. Further limitations were due to the rupture crossing unfavourable environments for stratigraphic interpretation (e.g. the valley-side fans that are crossed by

the rupture are too coarse, including those in Fig. 3), or following slopes where we could expect increased erosion rates, lack of appropriate material for dating and lack of stratigraphic features useful as piercing points in potential future 3D trenching.

Given the above, the final choice was a gentle scarp on a terrace of the Mudurnu River (Figs. 3, 4 and 5), based on: (a) the fact that the scarp was at the prolongation of a zone where larger cumulative scarps in older (valley-side fan) deposits were identified in 1:18,000 aerial photographs and in the field, coincident with the general trace of the 1967 rupture mapped by Ambraseys and Zatopek (1969), indicating that this has been a persistent fault trace in the recent past, (b) there was subsequent verification by eye-witnesses that the 1967 rupture was there and we also identified the scarp in one of the photographs of Ambraseys and Zatopek (1969) – Fig. 5a -, (c) small exposures of the terrace deposits indicated the presence of finer (sand and silt) layers and relatively small-calibre gravel (as opposed to boulders in other locations), (d) the vertical component of displacement at this location could be favourable for paleoseismic interpretation and (e) there was space to excavate and permission was granted by the owner.

A very detailed topographic survey of the trench site (Fig. 4) was carried out with a total station. The degraded coseismic scarp shown in Figs. 5a/b is well-expressed in the micro-topography (scarp S1), with a max. height of 0.8-1 m, superimposed on a broader ground flexure. The terrace surface behind scarp S1 appears to be back-tilted, whereas subtle arching is also possible (erosion to the S of the scarp has altered the purely tectonic morphology, not permitting a firm conclusion).

Scarp S1 is interrupted by a N-S trending, very subtle erosional feature (R1, essentially a very gentle terrace riser) which may have formed either by a tributary stream coming from the S or from the Mudurnu R. itself. To the W of riser R1, a much lower scarp (S2) is recognized at the prolongation of scarp S1. The transition between the two is abrupt, whereas the terrace surface is much flatter to the S of scarp S2 than S of S1. This

contrast across R1 suggests that at least two earthquakes have affected the terrace, separated by incision of the deformed terrace surface and formation of R1.

To the E and W of scarps S1 and S2, we could not pinpoint the exact location of the 1967 rupture. A possible case of offset channel was found to the W, whereas to the E a gentle WNW-ESE scarp was identified in the aerial photographs (S3 in Fig. 4), just N of which smaller gentle scarps and depressions with more E-W trends were seen in a field where there has been man-made modification also. A marked anomaly on the riser cut into the valley-side alluvial fan (R2), most probably also coincides with a splay of the fault. Which of these features hosted ruptures in 1967 could not be clarified though, due to conflicting eye-witness accounts.

Due to logistical reasons, our reconnaissance trench had to be excavated before the micro-topographic survey, not suspecting the existence of riser R1. The site was chosen to be away from obvious along-scarp modification and because of a small depression in front of scarp S2, a feature which, if tectonic and repeating in older earthquake ruptures: (a) might have been a trap for finer (overbank) deposits and (b) a location of increased wetness (given the shallow water table) with marsh vegetation producing in situ organic matter (desirable for dating), whereas (c) would increase chances of distinguishing paleoearthquakes (e.g. Weldon et al. 1996) corresponding to a structure with more fault splays (negative flower structure, e.g. Sylvester 1988)

General stratigraphic and tectonic features of the trench

The trench was 30 m long, ~2 m wide and up to 2.25 m deep (limited by the water table). Both walls were accurately gridded, with vertical lines at irregular intervals to avoid coincidence with fault zones or, anomalous parts of the wall where photo-mosaicing would

be problematic. Image warping software was used for on-site construction of high-resolution photo-mosaics, which were used for logging in 1:10 scale.

A suite of gravel-dominated, river channel deposits, capped by a 10-50 cm deposit of brown colluvium were exposed (Figs. 6 and 7), crossed by three parallel fault zones (FZ1 to 3). Discrete faulting of the upper part of the stratigraphy was observed in FZ1, which coincided with the gentle N-facing surface scarp S1 (Fig. 5), and FZ3. FZ2 was sealed. The depression in front of S1, the reason to select the specific place for the trench, proved to be an erosional feature, not corresponding to deformation of the underlying strata.

The recently active fault zones 1 and 3 were the boundaries of a very subtle ridge morphology at the surface (Figs. 6 and 7, more pronounced on the E wall). Such fault-parallel tectonic ridges are common in strike-slip zones, at various scales (e.g. Flemming and Johnson 1997) and were documented also along several stretches of the 1967 rupture by Ambraseys & Zatopek (1969). They are bound by fault splays on either side and, as in our case, may be parts of composite morphotectonic features, superimposed on scarps formed by vertical offset across the fault zone (e.g. Flemming and Johnson 1997; Pucci et al. 2006).

Simplified logs of the trench walls are given in Fig. 7a/b and brief descriptions of stratigraphic units in Table 1. The general stratigraphic configuration is given in Fig. 6a. The youngest unit group was a well-defined channel rich in fine sands (A), trending parallel to FZ1 (Fig. 6b). Its relatively lower-energy deposits suggest either a secondary channel of the Mudurnu R. or a tributary stream. Channel A was cut into different deposits across FZ1. From FZ1 to the N, it overlies a larger channel filled by S-dipping pebble and coarse sand layers (C). On the S side of FZ1, channel A overlies a small slice of another FZ1-parallel channel (B) and an extensive unit of coarse sands, pebbles and cobbles (E). At the central part of the trench, E consisted of S-dipping, well-sorted cross-beds (Figs. 7a/b,

9 and 10, true dip approx. SW), a structure suggesting lateral accretion inside a large channel of the Mudurnu R. (possibly a bar deposit - e.g. Friedman and Sanders 1978; Reineck and Singh 1973). Package E was overlying bedload deposits (coarse pebbles and cobbles) of the Mudurnu R. that extended all across the bottom of the trench, with different sub-units juxtaposed by the 3 fault zones (Z – Fig. 6a). The monotony of the gravel below E was interrupted between fault zones 2 and 3, where a suite of channels was found (F, G, H and J in Fig. 6a). Channel H was filled with a variety of materials in sub-channels, but predominant were sands with large-scale cross-bedding (mega-ripples or small aqueous dunes, H5a/b in Figs. 7d and 9), suggesting deposition in a substantially deep channel (e.g. Collinson and Thomson 1982), which we attribute to the Mudurnu R. rather than a tributary stream. Across FZ3 on the E wall, package E was progressively fining towards the S, changing also in internal structure. On the W wall it was giving way to unit group D, which consisted of smaller calibre gravel intercalated in sandy silt, materials that may have been deposited by a tributary stream coming from the S.

Fault zones and paleo-earthquake recognition

Fault zone 1

Mismatch of units in channel A and disappearance of channel B across FZ1 in both walls (Figs. 7a-c), indicates that the FZ1 has hosted important horizontal displacement, thus, the displacement mechanism cannot have been gravitational failure, expected perhaps since the scarp and trench were near the edge of a terrace (Fig. 4). On the E wall, FZ1 is expressed as a V-shaped structure, with strands converging downwards at the top of units

Z1-Z2 (Fig. 7c). The lower part of the "V" was occupied by a sheared mix of surrounding units (A6b-c), whereas the upper part (A6a) was fine sand and silt of unit A8, enriched in organic matter. The bounding fault strands could be clearly defined on the N side and the lower part of the S side. Dotted lines in Fig. 7c indicate possible other strands inside FZ1, whose true extents were masked by intense bioturbation.

The exposure on the W wall (Fig. 7b) was worse, due to predominance of fine sands and silt in the fault zone (unit A6d). The lamination inside unit A6d was almost completely destroyed, either due to liquefaction or, due to pedogenic alteration that resulted in a massive upper part of the unit, enriched in silt and organic matter (like A6a on the E wall). Large roots had also completely destroyed parts of the A6d stratigraphy. The southern bounding fault could be traced with certainty and parts of other fault strands were discernible inside the fault zone (offsetting gravel layers inside the sands), but were of no use to paleoseismic interpretation since their upward extents could not be defined unequivocally.

A noteworthy feature of FZ1 (but also of FZ2 and FZ3) was its non-visibility (Bonilla and Lienkaemper 1990; McCalpin 1996) in the lower gravel units (Z1/2, Fig. 8). We found no indications supporting an alternative interpretation involving bedding-plane slip (e.g. Bonilla and Lienkaemper 1990; Weldon et al. 2002). It seems that the exposure of units Z1/2 (53 cm above the trench floor and water table) was too small for the fault zone to be expressed in the specific type of material (coarse pebbles and cobbles in matrix of fine pebbles and very coarse sand without discernible stratification). If we assume that vertical displacement should be more favourable for the development of shear fabric, another reason might be the expectedly small amount of cumulative vertical displacement that the Z deposits have undergone.

Paleoearthquake recognition. According to two independent eye-witnesses of the 1967 rupture, FZ1 was associated with ground ruptures. All we could identify was small

discrete displacement of the bottom of the uppermost layer of colluvium (unit 1) on the northern main strand of the E wall. This lack of discrete displacements suggests that vertical component of the 1967 displacement was distributed in warping and discrete offsets too small to detect in the unfavourable deposits at hand. This was the style of the rupture a few tens of meters to the E, as seen in the photograph of Ambraseys and Zatopek (1969) –Fig. 5a-, with a predominantly flexural scarp and small discrete offsets distributed in several left-stepping small fault strands trending oblique to the direction of FZ1 (Riedel shears, e.g. Sylvester, 1988). Because our trench was located at the W termination of the scarp in Fig. 5a (where deformation was progressively dying out), we expect that both the total amount of flexure and the discrete displacements on Riedel shears were substantially smaller than those seen in Fig. 5a.

A well-defined paleo-earthquake (**FZ1-1**) took place before the deposition of unit A2, the horizontal erosional base of which truncated a package of deformed layers below it, forming an angular unconformity (Figs. 7c and 8). The deformed package was a triangular slice of sands and fine to medium gravel (units A16, A15, A14, A4 and A3), pushed up and warped in-between two very well defined strands of the fault zone. The outer (N) strand was associated with discrete displacement of correlative layers across it (A14 and A15) and was dying-out upwards (Bonilla and Lienkaemper, 1990). The main lamination surfaces (not subordinate cross-beds) inside the sands of the "slice", had attained abnormally steep dips (more than 40°). Such dips were not observed in the same package on the W wall, which was not faulted in the same style. It should be noted that, we do not define the event horizon based on the upper termination of the dying-out-upwards northern fault strand but, based on the overall picture of deformation (warping) below the non-deformed base of unit A2.

The base of channel A, which corresponds to the base of units A16 and A8-9, exhibited a vertical separation of ca. 50 cm across FZ1 on both walls. We estimate a

vertical separation of 35 cm across FZ1 for the base of unit A2, on the E wall. Given that: (a) channel A was perfectly parallel to FZ1 (Fig. 6b), (b) the bases of both channel A and unit A2 inside it had a quite regular shape on both walls and a very low dip to the W, we conclude that most of the observed vertical separation is not apparent, as is common in strike-slip faults, but true. Thus, we have a second, independent indication of at least one paleoearthquake inside channel A (FZ1-1), before the deposition of unit A2.

Based on the striking alignment of channel A with FZ1, we may propose that channel A was most probably established here after a scarp-forming paleoearthquake similar to 1967 and FZ1-1. This probable paleoearthquake (FZ1-2) would postdate the deposition of unit group E (into which A was cut). Channel A was super-imposed on channel B which, apparently also had an FZ1-parallel southern margin. This suggests that B was established first, after the inferred earthquake FZ1-2, followed by A at the same location. Thus we will put the event horizon for FZ1-2 below channel B (Fig. 7c).

Fault zone 2

Fault zone 2 (FZ2) was recognized at the lower part of the stratigraphy on the E wall, below channel H (Figs. 6a, 7d and 9). The fault strand that was discernible with certainty, was juxtaposing units J2 and 3 (channel J) against Z3 (Figs. 7d and 9). Unit J3 consisted of quite steeply S-dipping (32°) coarse sand layers that were fining down-dip to fine sands with intercalations of pieces of wood and abundant nut-shells and large spores. This down-dip fining can be considered anomalous, perhaps suggesting that the unit had been tilted towards the S. Bedding inside unit J3 was warped against the J2/3-Z3 fault contact, whereas re-orientation of pebbles of Z3 into a faint “shear fabric” was discerned after pushing the wall back a few cm. The lower part of unit J3 had been subjected to vivid

coloration, due to enrichment in greyish-blue clay coming from below, along the fault. In fact, a clay unit of exactly the same color was observed during the excavation. at a small depth below the water table at this part of the trench.

On the W wall, only a small occurrence of a sand unit that might correlate to unit J3 was seen just above the water table (Fig. 7b). This sand unit had the same coloration as J3 and was in sharp contact (10 cm exposure above the water) with a package of Z3 gravel to its N, the clast orientations inside which appeared disturbed, hence the dashed fault with question-mark at metre 18 in Fig. 7b. We consider it possible that a second strand of FZ2 existed about 1m to the N (metre 17), where a change in the calibre and bedding of the Z gravel was observed, a boulder about 1m coinciding with the transition from Z3 to the coarser Z2.

Paleoearthquake recognition. The base of unit H5b (the base of channel H) was continuing undisturbed across the recognized fault on the E wall, for at least 20 cm to the N. Furthermore, a thin layer of gravel at the base of H5b (drawn with dashed line in Fig. 9), was discernible also across the lower part of root zone R1, with root-stirred and silt-enriched H5b sands above it (R1' in Fig. 9). Small rootlets observed at the upward prolongation of the fault (not drawn in the figures) suggest that cracking through H5b may have taken place but, this was definitely a very minor feature compared to the sharp contrast across the fault below H5b (J2-3 juxtaposed against Z3). In addition, on the W wall where roots were not obscuring stratigraphic relationships, the base of H5b was well-expressed as a continuous and undisturbed contact. Thus, our interpretation is that unit H5b was sealing the recognised fault on the E wall and we place a paleoearthquake (FZ2-1) after unit group J and before H5b. It is likely that deformation of the ground into a S-facing, possibly flexural scarp by this earthquake (possible flexure being responsible for tilting of unit J3 to the S), was responsible for the establishment of the N margin of channel H, which trends parallel to FZ2 (as indicated from its well-defined shape in both walls).

Fault zone 3

Fault zone 3 corresponded to the S edge of the ridge morphology observed at the surface profile of the E wall and consisted of two main strands on both walls (Figs. 7a/b and 10), bounding a zone across which marked lateral changes were observed in the stratigraphy. As in all other cases, in the lower gravel (Z), no unambiguous indication of the FZ could be discerned.

On the E wall, the N strand of FZ3 was clearly expressed at meter 21, juxtaposing markedly different units and offsetting the base of the surface colluvium (unit 1 in Figs. 7d and 10). The S strand (meter 22) was identified based on a conspicuous sub-vertical orientation of coarse pebbles and cobbles near the S boundary of unit G2 (Figs. 7d and 10). On the W wall (Fig. 7b), the bounding faults could be traced with certainty at the upper part of the stratigraphy where they were juxtaposing contrasting units, e.g. gravel against silt (units E1/D2). Parts of several faults could also be traced inside the fault zone.

A most characteristic feature related to FZ3 is the absence of the large channel margin G1 on the W wall (Fig. 6, very well defined in Fig. 10). This cannot be attributed to erosion, since older units belonging to group H are preserved below unit E1, at the same height were G1 would be expected. Thus, we conclude that channel G1 was trending oblique to FZ3 (~ NE-SW or NNE-SSW trend) and has been offset more than the trench width (~ 2m). Unit G2, part of the same channel as G1, was also clearly absent on the W wall. This suggests a complex fault pattern, and not a 1-to-1 correlation of the bounding fault strands on the two walls. The fault strands are expected to trend oblique to the zone general direction (e.g. Ambraseys and Zatopek 1969; Sylvester 1988; Pucci et al. 2005).

Paleoearthquake recognition. The offset of the base of the surface colluvium (unit 1) by the N strand of FZ3 on the W wall. combined with the most detailed eye-witness account that mentioned a second rupture a few meters to the S of the surface scarp (FZ1), suggest that the N strand of FZ3 ruptured in 1967. On the W wall, both strands of FZ3 were clearly affecting the upper unit groups with appreciable horizontal offsets, judging from the juxtaposition of different unit groups (E and D). Still, the FZ3 strands were sealed by the base of unit 1 (Fig. 7b), suggesting that the 1967 rupture died out laterally here and that also a pre-1967 event (**FZ3-1**) had affected unit groups E and D. FZ3 was also the S limit of a subtle, but distinct arching of the top of unit group E. This arching was not clearly expressed at the surface as in the E wall, presumably due to westward dying-out of the deformation, coverage by unit 1 and, subsequently, ploughing by man.

The S strand of FZ3 on the E wall, corresponded only to a crack across units F2 and E2 above it, as suggested by very loose gravel and two roots (Fig. 10). The S-dipping gravel beds of E2 were clearly continuous across it (in Fig. 11, small bends of these beds are apparent, due to embayments of the wall formed by collapses along the crack). We consider the case of die-out upwards unlikely, given the large size of the re-oriented clasts inside G2, which suggests deformation that should be visible at the fairly well defined base of F2. Thus, we favour an event (**FZ3-2**) before the deposition of unit F2 and after the deposition of unit G1/2 (channel G). On the W wall, although several faults could be identified, recognition of paleoevents was not possible: faults either went all the way to the base of unit 1, or their upward extents could not be defined, going through unfavourable deposits (unit D2 – bio-turbated, massive silt with very coarse sand and very fine pebbles).

Synthesis of paleoseismic evidence

Based on the stratigraphic relationships of units post- and pre-dating the paleoearthquakes identified on the three individual fault zones, we recognise at least three different surface-faulting paleoearthquakes (prior to the 1967 earthquake) for the rupture zone as a whole. One extra event is possible, suggested by indirect evidence. In more detail, paleoearthquake **I** is event FZ1-1 that affected the deposits of channel A and, together with the possible event FZ1-2 (**II**), is younger than unit group E (Fig. 7c). The pre-1967 event suggested at FZ3 on the W wall (FZ3-1, Fig. 7b) cannot be discriminated from I and II. Event FZ3-2 (**III**) occurred before the deposition of unit group E and after the formation of channel G (Fig. 7d). Event FZ2-1 (**IV**) is older than FZ3-2 (III), since it occurred before the establishment of channel H, into which channel G was cut (Fig. 7d).

We note the possibility of under-representation of the paleoseismic history (e.g. McCalpin 1996) in the sedimentary environment of the trench, the main reason being that erosion can easily eradicate -and has done so- paleoseismic evidence. E.g. the upper part of FZ2 has been eroded away, leaving only a single strand at the bottom of the trench, whereas the establishment of channel A over FZ1, resulted in erosion of all stratigraphic evidence of pre-I events (e.g. the indirectly defined event II). Other causes of under-representation can be the destruction of paleoseismic evidence from bio-turbation or shaking-induced disturbance by subsequent events (e.g. in the fine sands of channel A that occupy most of FZ1) or, our inability to understand the extents of fault strands through homogeneous deposits (e.g. FZ3, W wall).

Radiocarbon Dating

In situ organic material was not found in the trench, with the exception of small gastropod shells in the clay and silt of H1. Given that limestones are abundant in the area, older apparent ages were to be expected from the shells due to hard-water effect (e.g. Weldon and Sieh 1985; Trumbore 2000), so they were not preferred over transported material (that would also give maximum ages for the enclosing layers). In addition, the distribution of detrital charcoal or pieces of wood, was far from ideal. Of the samples collected, those chosen for dating (Table 2, locations in Fig. 7c and d) were from the lower stratigraphic units, for the purpose of constraining the time interval during which the identified paleoearthquakes took place.

In order to constrain the timing of paleoearthquake I, we dated a large piece of charcoal from the bottom of channel A (sample W35, from unit A16 - Table 2). The analysis of the sample yielded more ^{14}C than the AD 1950 reference standard (reported in “pMC” in Table 2 - "percent modern carbon"). This generally means that the plant from which the sample came must have been respiring carbon after ~AD 1950. We can safely exclude that this may be the age of unit A16. We consider it very unlikely that the sample was a root, plus, we had no indications of possible contamination of W35 (no roots nearby, apparently no alterations of the enclosing sands). We note that when the lower limit of the 2 sigma pMC value range extends below 100% (99.6% in our case) there is some probability for 18th, 19th, or 20th century antiquity (laboratory report). This would suggest that the penultimate event may have occurred anytime between ca. AD 1700 and 1967. Yet, this age being unpaired, it would not be prudent to exclude the possibility that the penultimate event may have been the earthquake of 1668 as suggested by Ikeda et al (1991) or, one of the earthquakes that followed the main 1668 event (see Ambraseys and Finkel 1995).

Sample E30 (calibrated age of AD 1220-1410 – Table 2) was a large piece of charcoal inside the fine deposits of unit X1, dated to constrain paleoearthquakes III to I.

Sample E31 from unit X2 (with little doubt, correlative to X1 across FZ3) was dated for cross-checking and yielded a younger conventional age that calibrates to AD 1394-1668. Given that both E31 and E30 were transported material, we will consider the age range of the youngest sample (AD 1394-1668, sample E31) as a maximum for the true age for unit X1. This way, the occurrence of events III to I is constrained to be for sure after AD 1394.

Sample E100 was pieces of nut-shells and large spores that were inter-bedded in the sands of unit J3, dated in order to constrain the timing of event IV (FZ2-1). The high concentration of this material suggested that they were derived from a source (a tree) nearby the site of deposition, thus, their age should be very close to the time of deposition of unit J3. One out of three different pieces was selected by the dating laboratory and yielded a calibrated age younger than AD 1693 (with 70% probability, between 1812-1919 – Table 2). Given that roots were abundant above the sample, which was also not charred, contamination by humic acids is possible. Thus, we also dated a piece of charcoal (E8 - flat, oriented parallel to bedding, with rounded edges, thus very unlikely to be a piece of root) that we collected from a part of J3 away from the main root concentration (also, not colored). We got an older conventional age, which suggests that events IV to I occurred for sure after ca. AD 1668 (44% probability), whereas there is 37% probability that they occurred after AD 1797. We note that the older age of E8 on its own does not necessarily indicate that E100 was contaminated, since both are transported material.

Because (a) we cannot absolutely exclude that E8 may have also been contaminated, since it was close to the water table in a permeable unit and ,not far from sample E100, (b) we did not have datable material from the gravel of units Z2 or Z4, to compare with the above ages from channel J, and (c) the relationship of the dated unit X1/2 to J could not be clarified[1], we will avoid proposing a unique interpretation of the

[1] [For the reviewer] In specific, we could not understand whether X1 belonged to channel H (in which case it would post-date J), due to the unclear nature of units 200 and 200a. Unit 200 was a mix of materials, intensely bio-turbated by roots (only the largest root-fills are drawn in the figures), inside what

radiocarbon dating results and thus, in the following we discuss two possible scenarios for earthquake recurrence.

Scenarios for earthquake recurrence

Since we do not really know whether the younger maximum ages obtained for the fill of channel J were the result of contamination or not, we will propose two respective scenarios for surface-rupturing earthquake recurrence (1 and 2 in Table 3). Different variants of these scenarios are derived if we include (or not) the possible extra paleo-earthquake (II) suggested by indirect evidence (1a and 2a in Table 3). For each scenario, a range of maximum values for the average recurrence interval (ARI hereafter) is given (range, based on the age range of the sample, and maximum, because the dated material is transported, thus providing maximum-limiting ages for the enclosing units). The maximum ARI values are calculated by subtracting the respective maximum-limiting ages from 1967 and dividing the difference by the number of pre-1967 earthquakes. Individual recurrence intervals may be substantially larger or smaller than the average values in Table 3, due to

---

could be the disturbance zone of an older large root. Furthermore, it is possible that the tongue-shaped U200a was a burrow-fill, similar to the –smaller- ones observed into unit H1 (drawn in black in Fig. 7d, see also Fig. 10). The latter are filled with similar coarse deposits from unit F2 (including pebbles) and are elongated along the sole of unit H1, which, being fine and thus more compact and stable (as X1 also is), was a suitable ceiling for a burrow.

That X1 might not have been a deposit inside channel H, seems to be supported (but cannot be proved) by the following: (a) it was a deposit that suggests slow accumulation of fine sediment, which typically occurs in marginal swamps (environments typifying the abandonment of channels), (b) on the W wall, channel H was well preserved but unit X1 was not found inside it, even though it is quite extensive on the E wall, (c) on the E wall, X1 in all probability correlated to X2 across FZ3, whereas the channel H deposits (the sands and the clay that was capping them, a cover relatively resistant to erosion), were nowhere to be found. Erosion of the channel H sands and clay to the S of FZ3 cannot be excluded but, we can comment that the stretch of X2 shown in Fig. 7a had not been subjected to important erosion, judging from the fact that its top was parallel to the tilted-to-the-North bedding inside it. If the above were to be considered conclusive, both X1 and J would be below channel H, thus leaving open the possibility that X1 was after all older than J. In such a case, the ages obtained for units X1/2 would constrain event IV also.

clustering of earthquake ruptures in time, a behaviour that has been identified e.g. by Okumura et al. 2005 on the neighbouring 1944 (Bolu) earthquake segment.

The most conservative scenarios are 1 and 1a in Table 3, in which we use the age of sample E31 from unit X1/2 as a constraint for the timing of events III to I. In these scenarios the younger ages for channel J are not considered, whereas the unknown relationship of unit X1/2 to channel J requires that the timing of event IV be unconstrained (even though it is possible that unit X1/2 may after all have been older than channel J and event IV). In this case, we have for sure two (possibly 3) paleoearthquakes after AD 1394 and before the 1967 earthquake (max. ARI 286 yrs, possibly 191 yrs). If we take into account the whole age range for sample E31, we obtain max. ARI ranges of 286-150 (possibly 191-100 yrs) for two (possibly three) earthquakes before 1967 (Table 3).

In scenario 2 (and 2a), we accept the maximum age obtained for sample E8 (AD 1668) from unit J and use it to constrain all recognised events (IV to I). The age of E100 is not considered, since the sample was more likely prone to contamination than E8, being close to a root zone (see previous section). The obtained max. ARIs (Table 3) are 100 yrs (possibly 75 yrs), for three (possibly four) paleoearthquakes, respectively.

For comparison, for the nearby Bolu fault (last rupture in 1944) average recurrence intervals of 200-300 yrs or 250-300 yrs have been proposed by Okumura et al. (1993, 2002). More recent studies by Kondo et al. (2005) constrain the penultimate event to be after AD 1640 and correlate it to the main 1668 earthquake (Ambraseys and Finkel 1995), whereas they place two prior events between AD 1210-1460 and between AD 840-960 (which they correlate to a historical earthquake in 1035). Okumura et al. (2005) identified 5 pre-1944 earthquakes since AD 500±50 and earthquake clustering in time, with recurrence intervals that may be as short as 100 yrs, to over 700 yrs. Recurrence intervals of 210 and 280 yrs and characteristic slip are reported by Klinger et al. (2003) at the step-over between the Golcuk and Izmit-Sapanca (geometric) sub-segments of the Aug. 1999

ruptures (Fig. 2a). Rockwell et al. (2003) recognized two and three surface ruptures during the past 300 years (incl. 1999) at successive sub-segments of the 1999 rupture, the eastern of which (L. Sapanca, three ruptures) also experienced less slip in 1999, suggesting an intervening soft segment boundary. They also propose that partial rupture or incomplete strain release of geometric segments of the NAFZ is possible, resulting in more frequent earthquakes for those segments.

Studies suggesting short recurrence intervals for various segments of the NAFZ neighbouring the Mudurnu valley branch are not few. E.g., Ambraseys (2001) proposes that the earthquake of August 1999 may have been preceded by a similar event only 105 years earlier, in 1894. Tsutsumi et al (2002) and Emre et al. (2003) report 3 or possibly 4 surface-rupturing events on the Izmit sub-segment of the 1999 rupture (including the August 1999 rupture) since the 17th century (ARI 100-150 yrs), a result presumably superseding that in Toda et al. (2001) from the same trenches. Furthermore, Pantosti et al. (2004) recognized 3 events (incl. Nov. 1999) during the last ca. 300 yrs in trenches on the November 1999 Duzce rupture (Fig. 2a). At one site (Mengencik / Findikli area), people living next to the rupture recalled narratives of their grandparents about an earthquake rupture at the exact same location, ca. 100 years ago.

Based on the above and the possibilities allowed by the abundant historical earthquakes in the broader area of Fig. 2a, scenarios 2 and 2a (100 and 75 yrs max. ARIs, resp.) are not necessarily extreme. An implication of the ARIs derived from these scenarios is that the paleoearthquakes recognised in the trench, may not have been repetitions of the 1967 earthquake, at least not all of them. That is, the 1967 earthquake may not be characteristic *sensu* Schwartz and Coppersmith (1984). This is suggested by simple calculations in the following. According to Wells and Coppersmith (1994), the average slip during the 1967 earthquake was 1.63 m, calculated based on Ambraseys and Zatopek (1969) (for comparison, Pinar et al. 1996, report 1.7 m for the main sub-event). If we

assume a minimum of 1.6 m of displacement per event, based on the maximum ARIs we obtain (minimum) slip rate estimates of 16 and 21.3 mm/yr (scenario 2 and 2a, respectively). Assuming that GPS measurements are characteristic of the medium-term relative motion across the NAFZ, the above slip rate estimates can be considered unrealistic (for sure the 21.3 mm/yr for scenario 2a, our preferred variant), given that, of a total of ca. 22-25 mm/yr of motion across the whole NAFZ in this area (Straub et al. 1997; McClusky et al. 2000), according to Ayhan et al. (2001) up to 10 mm/yr are accommodated by the northern branch of the zone (Duzce-Karadere faults). Some unknown additional amount may also be distributed in smaller (secondary) structures, a fact that would further decrease the strain that remains to be accommodated by the Mudurnu branch of the NAFZ.

One possible reason for having so many surface ruptures in the short period of scenarios 2/2a at the particular stretch of the Mudurnu valley branch of the NAFZ where our trench was located, can be that successive ruptures like 1957 and 1967 may have overlapped at different areas in the past. Our trench could be in such a previous overlap area. Alternatively, it may be that we trenched a stretch (geometric segment) of the fault that hosts more frequent, smaller earthquake ruptures due to partial rupture or incomplete strain release, as suggested by Rockwell et al. (2003) based on their work in neighbouring parts of the NAFZ. Furthermore, our trench was located at an area where the relatively less active Iznik-Mekece branch (e.g. Straub 1997; Neugebauer 1997) of the NAFZ (Fig. 2) meets with the Mudurnu valley branch. The junction between the two is drawn as a clear-cut feature in some small scale maps in the bibliography (e.g. Michel et al. 1995), whereas it is dashed or not drawn in others (e.g. Neugebauer et al. 1997 and Herece and Akay 2003a, respectively). Judging from its geomorphic signature, it may be that the junction is an area where deformation is distributed to several faults. Thus, another possibility is that ruptures on the Iznik fault (the most recent one having occurred at 200-500 BP according

to Honkura and Isikara 1991) may have been accompanied by ruptures also in the Mudurnu valley.

Summary and conclusions

The paleoseismic interpretation of a trench located at the central part of the July 22, 1967 earthquake segment (Mudurnu valley), yielded preliminary constraints on the recurrence of recent surface-rupturing earthquakes at the southern branch of the NAFZ, W of the Bolu basin. The trench was excavated on a Holocene terrace of the Mudurnu River, across a N-facing scarp and a very subtle pressure ridge (push-up) about 12 m wide, superimposed on the scarp. The internal structure of the pressure ridge consisted of two bounding fault zones that were reaching the present surface and a sealed fault zone in-between them. When better sites are lacking, this type of configuration can be a point of advantage, since the cumulative deformation may be expected to be distributed in several structures, thus being easier to interpret. A key point is that trenches should be long enough to intercept all the fault zones that may be across and at the boundaries of the push-up, which, as in our case, may be only a very subtle and not immediately recognizable feature on the surface.

Three (possibly four) paleoearthquakes –before 1967- were identified in the trench (I to IV – Figs. 7c and d). The most conservative interpretation of the radiocarbon dating results (scenarios 1-1a in Table 3), suggests that at least two (possibly three) paleoearthquakes have occurred since AD 1394. This translates to a maximum average recurrence interval of 286 yrs (possibly 191 yrs), whereas the oldest recognised event (IV) is unconstrained. An unpaired radiocarbon age suggests that the penultimate event occurred after ca. AD1700, but one date may not be sufficient to exclude the possibility

that it may have been one of the earthquakes that occurred in 1668, or the main one, as suggested by Ikeda et al (1991).

A second interpretation (scenarios 2-2a in Table 3), which we cannot exclude with the available data, can be based on very young ages obtained from a unit affected by the oldest event recognised (IV). Two ages from different materials that for sure were not roots, suggest that paleoearthquake IV and the two (possibly three) younger ones occurred since ca. AD1668 (max. average recurrence interval 100 yrs, possibly 75 yrs). An implication of this second scenario is that the 1967 earthquake rupture may not be characteristic. This is so because a minimum value for the slip during this earthquake multiplied by (maximum) average recurrence intervals of 100-75 yrs, yields minimum values for the slip rate of the southern branch of the NAFZ that may be too high compared to those we can infer from GPS measurements (for sure, in the case of 75 yrs max. average recurrence interval).

Acknowledgements

This work was carried out in the frame of the European Union Project REL.I.E.F. (Reliable information on Earthquake faulting - EVG1-CT-2002-00069) under the auspices of the Istanbul Technical University and Assoc. Prof. Serdar Akyüz, whom we warmly thank for his invaluable support. We are grateful to Mr. Muhammet Kahraman, the land-owner and patient backhoe operator that excavated his field for this study, as well as the local authorities at Akyazi, and the people living in the Mudurnu valley, that were always willing to provide any information they could about the 1967 earthquake ruptures.

References

Akyüz, S., Hartleb, R. D., Barka, A. A., Altunel, E., Sunal, G., Meyer, B., and R. Armijo (2002) Surface rupture and slip distribution of the 12 November 1999 Duzce earthquake (M7.1), North Anatolian Fault, Bolu, Turkey, *Bull. Seism. Soc. Am*. 92, no. 1, 61-66

Ambraseys, N. N., and A. Zatopek (1969). The Mudurnu valley, West Anatolia, Turkey, earthquake of 22 July 1967, *Bull. Seism. Soc. Am*. 59, no. 2, 521-589.

Ambraseys, N. N. (1970). Some characteristic features of the Anatolian fault zone, *Tectonophysics* 9, 143–165.

Ambraseys, N. N. and C. Finkel (1995). *The Seismicity of Turkey and Adjacent Areas: A Historical Review, 1500–1800*, Eren Yayincilik ve Kitapcilik Ltd, Istanbu, 240 pp..

Ambraseys, N. N. and J. A. Jakson (1998). Faulting associated with historical and recent earthquakes in the Eastern Mediterranean region, *Geophys. J. Int.* 133, 390-406.

Ambraseys, N. N. (2001). The earthquake of 10 July 1894 in the Gulf of Izmit (Turkey) and its relation to the earthquake of 17 August 1999, *Journal of Seismology* 5, 117-128.

Ambraseys, N. N. (2002). The seismic activity of the Marmara sea region over the last 2000 years. *Bull. Seism. Soc. Am*. 92, no. 1, 1-18.

Ambraseys, N. N. (2004). *Revised earthquake Catalog for the period 1500 to present*., Reports of the "REL.I.E.F." E.U. project (EVG1-CT-2002-00069), deliv. 16, 29-60.

Atakan, K., Ojeda, A., Meghraoui, M., Barka, A., Erdik, M., and A. Bodare (2002). Seismic Hazard in Istanbul following the 17 August 1999 Izmit and 12 November 1999 Duzce earthquakes, *Bull. Seism. Soc. Am*. 92, no. 1, 466-482.

Ayhan, M., Burgmann, R., McClusky, S., Lenk, O., Aktug, B., Herece, E. and R. Reilinger (2001). Kinematics of the Mw=7.2, 12 November 1999, Duzce, Turkey earthquake, *Geophys. Res. Lett.* 28, no. 2, 367-370.

Barka, A. A., Akyüz, H. S., Altunel, E., Sunal, G., Cakir, Z., Dikbas, A., Yerli, B., Armijo, R., Meyer, B., deChabalier, J. B., Rockwell, T., Dolan, J.R., Hartleb, R., Dawson, T., Christofferson, S., Tucker, A., Fumal, T., Langridge, R., Stenner, H., Lettis, W., Bachuber, J. and W. Page (2002). The surface rupture and slip distribution of the August 17, 1999 İzmit earthquake, M=7.4, North Anatolian Fault, *Bull. Seism. Soc. Am*. 92, no. 1, 43-60.

Barka, A. A. (1996). Slip distribution along the North Anatolian fault associated with large earthquakes of the period 1939 to 1967, *Bull. Seism. Soc. Am*. 86, 1238-1254.

Barka, A. A. (1992). The North Anatolian fault zone. Annales Tectonicae 6, 164–195.

Bonilla, M. G. and I. J. Lienkaemper JJ (1990). Visibility of fault strands in exploratory trenches and timing of rupture events, *Geology* 18, 153-156.

Bozkurt, E. (2001). Neotectonics of Turkey - a synthesis, *Geodinamica Acta* 14, 3-30.

DOI:S098531110101066X/FLA

Collinson J.D. and D. B. Thomson (1982). *Sedimentary structures*, G. Allen & Unwin, London, 194 pp..

Demirtaş, R. (1996). Kuzey Anadolu Fayı'nın paleosismitesi: Mudurnu Vadisi segmentinde örnek çalışma (Paleoseismology of the North Anatolian Fault: A case study of the Mudurnu valley segment, NW Turkey), *Türkiye Jeoloji Kurultayı Bülteni* 11, 154-162.

Demirtaş, R., (2000). Kuzey Anadolu fay zonu'nun Abant-Gerede arasinda kalan Bolumunun neotektonik ozellikleri ve paleosismisitesi, *Doktora Tezi, Ankara Universitesi, Turkey,* 211 pp.

Emre, O., Toda, S., Duman, T. Y., Sugai, T., Dogan, A., Awata, Y., Okuno, M., Tsutsumi, H., Ozalp, S., and F. Tokay (2003). Recurrence of the large earthquakes on the 1999 Izmit and Duzce surface ruptures, North Anatolian Fault, Turkey, *EGS - AGU - EUG Joint Assembly Abstracts*, 4635

Flemming, R. W. and A. M. Johnson (1997), Growth of a tectonic ridge during the Landers earthquake, *Geology* 25, no. 4, 323-326.

Friedman, G. M. and J. E. Sanders (1978). *Principles of sedimentology*, John Wiley & Sons, New York, 792 pp.

Guidoboni, E., Comastri, A., Fanelli, G., Bianchi, M. G., Tarabusi, G. and A. Rigo (2004). *Collection, analyses and elaborations of historical records about earthquake effects in the North-Anatolian Fault between the Gulf of Saros and Bolu, from the 5th century B.C. to the 15th century A.D.* Storia Geofisica Ambiente, Bologna, Report 264/04, 138 pp. Also in: Reports of the "REL.I.E.F." E.U. project (EVG1-CT-2002-00069), appendix to deliv. 16

Herece, E., and E. Akay (2003a). *1:100.000 geological maps along the North Anatolian Fault – Sapanca-Dokurcun sheet*. General Directorate of Mineral Research and Exploration (MTA), Ankara.

Herece, E., and E. Akay (2003b). *1:100.000 geological maps along the North Anatolian Fault – Bolu sheet.* General Directorate of Mineral Research and Exploration (MTA), Ankara.

Honkura, Y. and A. M. Isikara (1991). Multidisciplinary research on fault activity in the western part of the North Anatolian Fault Zone, *Tectonophysics* 193, 347-357.

Ikeda, Y., Suzuki, Y., Herece, E., Saroglu, F., Isikara, A., and Y. Honkura (1991). Geological evidence for the last two faulting events on the North Anatolian fault zone in the Mudurnu valley, western Turkey, *Tectonophysics* 193, 335-345.

Ikeda, Y., Honkura, Y. and A.M. Isikara (1989). Quaternary compressional deformation in the Izmit-Sapanca Trough, W Turkey, and its implications for the presents tectonics near the W termination of the NAFZ. In: Honkura Y, Isikara AM (eds). Multidisciplinary Research on Fault Activity in the Western Part of the North Anatolian Fault Zone. Tokyo Institute of Technology, pp 1-162

Klinger, Y., Sieh, K., Altunel, E., Akoglu, A., Barka, A., Dawson, T., Gonzalez, T., Meltzner, Z., and T. Rockwell (2003). Paleoseismic Evidence of Characteristic Slip on the Western Segment of the North Anatolian Fault, Turkey, *Bull. Seism. Soc. Am.* 93, no. 6, 2317-2332.

Kondo, H., Ozaksoy, V., Yildirim, C., Awata, Y., Emre, O., and K. Okumura (2005). Slip history at Demir Tepe site the 1944 Bolu-Gerede rupture, North Anatolian Fault System, Turkey. Proc. Hokudan Intern Symp on Active Faulting, p. 69.

Langridge, R. M., Stenner, H. D., Fumal, T. E., Christofferson, S. A., Rockwell, T. K., Hartleb, R. D., Bachuber, G., and A. A. Barka (2002). Geometry, slip distribution, and kinematics of surface rupture on the Sakarya fault segment during the 17 August 1999 Izmit, Turkey, earthquake, *Bull. Seism. Soc. Am.* 92, no. 1, 107-125.

McCalpin, J. (1996). Field techniques in Paleoseismology. In: McCalpin J (ed). Paleoseismology. Academic Press, San Diego, pp 33-83.

McClusky, S., Balassanian, S., Barka, A., Demir, C., Ergintav, S., Georgiev, I., Gurkan, O., Hamburger, M., Hurst, K., Kahle, H., Kastens, K., Kekelidze, G., King, R., Kotzev, V., Lenk, O., Mahmoud, S., Mishin, A., Nadariya, M., Ouzounis, A., Paradissis, D., Peter, Y., Prilepin, M., Reilinger, R., Sanli, I., Seeger, H., Tealeb, A., Toksoz, M. N., and G. Veis (2000) Global positioning system constraints on plate kinematics and dynamics in the eastern Mediterranean and Caucasus, *J. Geophys. Res.* 105, no. 3, 5695–5719.

McKenzie, D. P. (1972). Active tectonics of the Mediterranean region, *Geophys. J. R. Astron. Soc.* 30, 109-185.

Michel, G. W., Waldhor, M., Neugebauer, J., and E. Appel (1995). Sequential rotation of stretching axes, and block rotations: a structural and paleomagnetic study along the North Anatolian Fault, *Tectonophysics* 243, 97-118.

Michel, G. W., and C. Janssen (1996). Deformation along an apparent seismic barrier: a paleoseismological study along the North Anatolian Fault, *Annali di Geofisica* XXXIX, no. 3, 647-662.

Muller, J. R., Aydin, A., and F. Maerten (2003). Investigating the transition between the 1967 Mudurnu valley and 1999 Izmit earthquakes along the North Anatolian fault with static stress changes, *Geophys. J. Int.*154, 471-482.

Neugebauer, J. (1995). Structures and kinematics of the North Anatolian Fault zone, Adapazari-Bolu region, northwest Turkey, *Tectonophysics* 243, 119-134.

Neugebauer, J., Loffler, M., Berckhemer, H., and A. Yatman (1997). Seismic observations at an overstep of the western North Anatolian Fault (Abant-Sapanca region, Turkey). *Geol. Rundsch.* 86, 93-102.

Okumura, K., Yoshioka, T., and I. Kuscu (1993). Surface faulting on the North Anatolian Fault in these two millennia, *U.S. Geol. Surv. Open-file Rep., 94-568*, 143-144.

Okumura, K., Awata, Y., Duman, T.Y., Tokay, F., Kuscu, I., and H. Kondo (2002). Rupture history of the 1944 Bolu-Gerede segment of the North Anatolian Fault: Gerede-Ardicli trench re-excavated, *AGU Fall 2002 Meeting Abstr.* S11B-1155.

Okumura, K., Rockwell, T.K., Kondo, H., Awata, Y., Duman, T. Y., and O. Emre (2005). The 1944 Bolu-Gerede segment of the North Anatolian fault. *Proc. of the 2005 Hokudan Intern Symp on Active Faulting*, p. 117

Pantosti, D., Pucci, S., Palyvos, N., Zabci, C., De Martini P. M., Uçarkus, G., Dikbas, A., Meghraoui, M., Akyüz, S., and P. Collins (2004). Paleoearthquakes along the Duzce fault segment of the North Anatolian Fault Zone, Turkey: preliminary results. *Proc. 32nd Int. Geol. Congr.*

Pinar, A., Honkura, Y., and M. Kikuchi (1996). A rupture model for the 1967 Mudurnu valley, Turkey earthquake and its implication for seismotectonics in the western part of the North Anatolian Fault Zone, *Geophys. Res. Lett.* 23, 29–32.

Pucci, S., Palyvos, N., Zabci, C., Pantosti, D., and M. Barchi (2006). Coseismic ruptures and tectonic landforms along the Duzce segment of the North Anatolian Fault Zone (Ms 7.1, Nov. 1999), *J. Geophys. Res.* (in press).

Reimer, P. J., Baillie, M. G. L., Bard, E., Bayliss, A., Beck, J. W., Bertrand, C. J. H., Blackwell, P. G., Buck, C. E., Burr, G. S., Cutler, K. B., Damon, P. E., Edwards, R. L., Fairbanks, R. G., Friedrich, M., Guilderson, T. P., Hogg, A. G., Hughen, K. A., Kromer, B., McCormac, F.G., Manning, S. W., Ramsey, C. B., Reimer, R. W., Remmele, S., Southon, J. R., Stuiver, M., Talamo, S., Taylor, F.W., van der Plicht, J., and, C. E. Weyhenmeyer (2004). IntCal04 Terrestrial radiocarbon age calibration, 26 - 0 ka BP, *Radiocarbon* 46, 1029-1058.

Reineck, H. E., and I.B Singh (1973). *Depositional sedimentary environments*. Springer-Verlag, Berlin, 439 pp.

Rockwell, T., Aksoy, E., Ferry, M., Klinger, Y., Langridge, R., Meghraoui, M., Meltzner, A., Ragona, D., Seitz, G., and G. Ucarkus (2003). Paleoseismic record of surface ruptures of the western third of the North Anatolian fault: Implications for fault segmentation models, *EGS - AGU - EUG Joint Assembly Abstr.* 13320.

Şaroğlu, F., Emre, Ö., and İ. Kuşçu (1992). *Active fault map of Turkey*, General Directorate of Mineral Research and Exploration (MTA), Ankara.

Schwartz, D. P., and K. J. Coppersmith (1984). Fault behaviour and characteristic earthquakes – examples from the Wasatch and San Andreas fault zones. *J. Geophys. Res.* 89, 5681-5698.

Şengör, A. M. C. (1979). The North Anatolian transform fault: Its age, offset and tectonic significance, *J. Geol. Soc. London* 136, 269-282.

Şengör, A. M. C., Tuysuz, O., Imren, C., Sakinc, M., Eyidogan, H., Gorur, N., Le Pichon, X., and C. Rangin (2004). The North Anatolian Fault: a new look. *Ann. Rev. Earth Planet Sci.* 33, 1-75. DOI: 10.1146/annurev.earth.32.101802.120415

Sieh, K. E. (1978). Prehistoric large earthquakes produced by slip on the San Andreas fault at Pallet Creek, California, *J. Geophys. Res.* 83, 3907-3939.

Sieh, K. E. (1996). The repetition of large-earthquake ruptures, *Proc. Natl. Acad. Sci. U.S.A.* 93, 3764-3771.

Stein, R. S., Barka, A. A., and J. H. Dieterich (1997). Progressive failure on the North Anatolian fault since 1939 by earthquake stress triggering, *Geophys. J. Int.* 128, 594-604.

Stuiver, M., and P. J. Reimer (1993). Extended 14C database and revised CALIB radiocarbon calibration program, *Radiocarbon* 35, 215-230.

Straub, C., Kahle, H. G., and C. Schindler (1997). GPS and geologic estimates of the tectonic activity in the Marmara Sea region, NW Anatolia, *J. Geophys. Res.* 102, no. B12, 27,587-27,601.

Sylvester, A. G. (1988). Strike-slip faults, *Bull. Geol. Soc. Am.* 100, 1666-1703.

Toda, S., Tsutsumi, H., Duman, T. Y., Emre, O., Okuno, M., Ozalp, S., Tokay, F., Dogan, A., Haraguchi, T., Kondo, H., Sugito, N., Nakamura, T., Parlak, O., and R. Ciplak (2001). Recurrence Interval of the Izmit-Type Earthquakes along the Western North Anatolian Fault, *AGU Fall 2001 Meeting Abstr.* S52C-0650.

Trumbore, S. E. (2000). *Radiocarbon Geochronology*. In: Noller, J. S., Sowers, J. M., and W.R.Lettis (eds), *Quaternary Geochronology: methods and applications*, AGU, Washington DC, Reference shelf 4, pp 41-60.

Tsutsumi, H., Toda, S., Emre, O., Okuno, M., Ozalp, S., Yildirim, C., Takada, K., and T. Nakamura (2002). Recurrence of Large Earthquakes on the 1999 Izmit Surface Rupture, North Anatolian Fault, Turkey, *AGU Fall 2002 Meeting Abstr.* S11B-1152.

Weldon, R. J., and K. E. Sieh (1985). Holocene rate of slip and tentative recurrence interval for large earthquakes on the San Andreas Fault, Cajon Pass, southern California, *Geol. Soc. Am. Bull.* 96, 793-812.

Weldon, R. J., McCalpin, J., and T. K. Rockwell (1996). Paleoseismology of strike-slip tectonic environments. In: McCalpin J (ed). Paleoseismology. Academic Press, San Diego, pp. 271-329.

Weldon, R. J., Fumal, T. J., Powers, S. K., Pezzopane, K. M., Scharer, K. M., and J. C. Hamilton (2002). Structure and earthquake offsets on the San Andreas Fault at the Wrightwood, California, paleoseismic site, *Bull. Seism. Soc. Am.* 92, no. 7, 2704-2725.

Wells, D. L., and K. J. Coppersmith (1994). New empirical relationships among magnitude, rupture length, rupture width, rupture area, and surface displacement, *Bull. Seism. Soc. Am.* 84, 974-1002.

Yeats, R., Sieh, K., and C. Allen (1997). *The geology of earthquakes*, Oxford University press, 568 pp.

Unit Group	Unit	Description
-	**1/1a**	1: Dark brown silt with pebbles (not bedded). 1a: ploughed upper horizon
A	**1**	Fine sand, silt and fine pebbles, bio-turbated and enriched in organic matter at its upper part
A	**2/2a**	Pebbles and cobbles in matrix of fine pebbles (2) and sand (2a)
A	**3 / 4**	Laminated fine (3) and medium (4) sand
A	**5**	Laminated medium/coarse sand, interfingering with pebbles (up to medium pebbles)
A	**6a-c**	[E Wall] (6a): Pedogenic alteration of unit A8 above fault zone 1. (b,c): Mixture of sheared units inside fault zone 1
A	**6d**	[W Wall] Root-stirred (and liquefied?) A8 sands and gravel. Pedogenic alteration and enrichment with organic matter at the upper part
A	**8**	[E wall]: Laminated fine / medium sand (same as A3, 4 and 5). [W wall]: Laminated fine / medium sand with pebble intercalation.
A	**9**	Very coarse pebbles in matrix of coarse sand/very fine pebbles
A	**12**	Medium pebbles in matrix of very fine pebbles and coarse sand
A	**13 / 13a**	(13): Bedded coarse sands grading to very coarse pebbles. (13a): Laminated medium/fine sands
A	**14**	Medium pebbles in matrix of coarse sand/very fine pebbles
A	**15**	Pebbles up to small cobbles in matrix of coarse sand/very fine pebbles
A	**16**	Laminated fine / medium sand with silt intercalations. Layer containing very coarse pebbles at its base.
A	**17**	Pebbles and small cobbles in matrix of coarse sand / very fine pebbles
B	**1**	Medium to coarse pebbles in matrix of coarse sand and very fine pebbles
B	**2**	Pebbles and small cobbles in matrix of sandy silt
C	**1/2**	Pebbles (up to very coarse) (1), grading laterally to coarse sands (2)
	45	Well-sorted, bedded fine / medium sand, grey color.
D	**1**	fine to coarse pebbles, coarse sand
D	**2**	Silt and very coarse sand/very fine pebbles
E	**1 - 3**	(1/2): Alternating layers of coarser or finer pebbles and cobbles in matrix of fine pebbles and coarse sand. Well-defined beds with apparent dip to the S (1). (3): generally finer than 1 and 2 (coarse sand and fine pebbles dominant, grading up to coarse pebbles)
F	**1-3**	Coarse sand (1); coarse sand with coarse pebbles and cobbles (2); pebbles and cobbles in silt matrix (3)
G	**1**	Well-sorted very coarse pebbles and small cobbles. Orange colored pebbles (by oxidation).
G	**2**	Small boulders, cobbles and pebbles in silt. Orange colored (oxidation).
H	**1**	Clay and silt, light brown colored
H	**2**	Coarse sands and fine pebbles with orange oxidation mottles
H	**3/4**	coarse pebbles and small cobbles, in coarse sand (3) / silt (4)
H	**5a/b/c**	Laminated fine sand, yellowish colored, large scale cross-bedding in a and b.
H	**5d**	Medium and coarse sand
H	**5e**	Fine to coarse well-sorted pebbles in matrix of sand and silt. N-dipping cross-beds
H	**5f**	coarse pebbles in silt
-	**57**	fine to coarse pebbles in silt
X	**1 /2**	Silt, with clay and very fine sand (1), Laminated silt and clay and very fine sand (2)
J	**1-3**	(1): Medium sands with trough cross-bedding, intensely bioturbated near FZ2 (2). (3): Medium to coarse sands, grey color, laminated, lower part colored greyish blue from underlying grayish blue clay layer. Nutshells, spores and pieces of wood interbedded with the sands at the lower part.
Z	**1**	Pebbles, cobbles and boulders in matrix of very coarse sand and fine pebbles
Z	**2-4**	Coarse pebbles and cobbles in matrix of fine pebbles & coarse sand
-	**200**	Pebbles in coarse sand matrix, disturbed by bioturbation (old roots or burrows infilled with silt)

-	**200a**	Pebbles in coarse sand matrix (filling a burrow?)

Table 1. Descriptions of stratigraphic units encountered in the trench, following the Wentworth grain size classification.

Sample code & Lab No.	**Material / Stratigraphic Unit**	**$^{13}C/^{12}C$ ratio**	**Measured R/C age (yr BP)**	**Conv. R/C age ($^{13}C/^{12}C$ corr.)**	**2 σ (95.4%) calibrated age (Calendar years)**
W35 Beta – 196473 (*)	Large charcoal piece (~2x2x2cm) (unit 17)	-21.8 ‰	100.7 ± 0.5 pMC (AMS)	100.1 ± 0.5 pMC	younger than ca. AD 1700
E100 Beta – 196472 (*)	Nutshell (not charred) (unit 80)	-25.1 ‰	30 ± 40 BP (AMS)	30 ± 40 BP	younger than AD 1693 [AD 1693-1728] probability:0,223797 [AD 1812-1919] probability:0,724322
E8 Beta – 199400 (*)	Flat, sub-rounded charcoal piece (2x3x0.5 cm) (unit 80)	-25.5 ‰	150 ± 40 BP (AMS)	140 ± 40 BP	younger than AD 1668 [AD 1668-1782] probability: 0,447087 [AD 1797-1893] probability: 0,37959
E31 Beta – 201527 (*)	Large charcoal piece (~2x2x4 cm) (unit 58)	-23.3 ‰	360 ± 90 BP Std. method / extended counting	390 ± 90 BP	AD 1394 – 1668
E30 Beta – 196471 (*)	Very large charcoal piece (~10x5x5 cm) (unit 58)	-27.6 ‰	730 ± 70 BP Std. method	690 ± 70 BP	AD 1217 – 1408

(*) Beta Analytic Inc., Miami, Florida, USA 33155

Table 2. Radiocarbon ages of dated samples (stratigraphic locations in Figs. 7c and d). Calibrations with the CALIB v. 5.0 software (Stuiver and Reimer, 1993) and calibration curves by Reimer et al. (2004).

Eearthquake	Timing Scenario 1	Timing Scenario 1a	Timing Scenario 2	Timing Scenario 2a
1967	AD 1967	AD 1967	AD 1967	AD 1967
I	MLA range AD1394-1668	MLA range AD1394-1668	After ~AD 1668	After ~AD 1668
II (Possible)	-	MLA range AD1394-1668	-	After ~AD 1668
III	MLA range AD1394-1668	MLA range AD1394-1668	After ~AD 1668	After ~AD 1668
IV	Dating failed	Dating failed	After ~AD 1668	After ~AD 1668
Max. Average recurrence interval	**286 -150 yrs**	**191-100 yrs**	**100 yrs**	**75 yrs**
Comments:	E100/E8 ages rejected	Same as 1 and event II accepted	E8 max. age accepted	Same as 2 and event II accepted

Table 3. Summary of recognized paleoearthquakes and two different scenarios about their timing. The most conservative ones are 1 and 1a. Scenarios 1a and 2a include a paleoearthquake (II) suggested by indirect evidence. MLA range: maximum-limiting age range.

FIGURE CAPTIONS

Figure 1. The North Anatolian Fault Zone (NAFZ) and the regional geodynamic setting (adapted from Atakan et al., 2002, with reference to Ambraseys, 1970, Barka, 1996 and references therein). The Anatolian (Asia Minor) micro-plate is escaping westwards due to the collision of the Arabian plate with Eurasia, a motion that is accommodated by the NAFZ and the East Anatolian Fault Zone (EAFZ). Thick lines indicate the segments of the NAFZ that have ruptured in this century. Magnitude and year of earthquakes are indicated in squares.

Figure 2. (a) The main structures of the NAFZ between Bolu and Izmit bay. Background DEM is not projected. Solid and dashed lines are certain and probable fault traces, respectively. Faults are predominantly dextral strike-slip, with differing amounts of vertical component of displacement. Black and white stars mark the geometric segments that ruptured during the Aug. 1999 and Nov. 1999 earthquakes, redrawn from Barka et al. (2002) and Akyüz et al. (2002), respectively. Faults compiled from Şaroğlu et al (1992), Neugebauer (1995) and Herece and Akay (2003a/b) with minor modifications and additions. Mainly faults that have a geomorphic expression (thus have been active in the Late Pleistocene-Holocene) are portrayed. Grey rectangle: Figure 2b. Question marks indicate uncertainty in the locations of the terminations of the 1944, 1957 and 1967 earthquake segments.

(b) Solid lines: the July 22, 1967 Mudurnu valley earthquake ruptures, as mapped in detail by Ambraseys and Zatopek (1969). Background DEM in UTM projection. Dotted lines: traces of faults from the literature or based on their geomorphic signature. The fault swarm at the W part of the area is generally associated to folding (Ikeda et al., 1989). Question-marks indicate uncertainty in the location of the E end of the Iznik-Mekece branch of the NAFZ (drawn at its NE part based on Michel et al., 1995, and outside their map, along a major lithological boundary that is found at the prolongation of their fault trace, but is not considered as a fault in Herece and Akay, 2003a). Another possible fault trace could be along the river just to the SE of the drawn trace.

Figure 3. Geomorphological sketch map of the Mudurnu river valley east of Beldibi village, based on 1:18,000 aerial photo interpretation and field reconnaissance. White color: unmapped areas. The 1967 rupture trace is drawn based on GPS points taken during our field reconnaissance (July 2004) and the trace of Ambraseys and Zatopek (1969). Numbers are referring to locations where the exact rupture trace was indicated to us in the field by eye-witnesses. Ellipse and question marks indicate an area where we were not able to locate the 1967 rupture.

Figure 4. Microtopographic map of the trench site plotted over an aerial photograph of the site, based on ca. 1500 points surveyed with total station. Elevation contours every 20 cm. The 1967 rupture was following scarps S1 and S2 (see Figure 5). For other explanations see text.

Figure 5. (a) The coseismic scarp (S1 in Fig. 4) at the trench shortly after the July 22, 1967 earthquake (photo from Ambraseys and Zatopek 1969). The orientation of the photograph mentioned in the photo caption in Ambraseys and Zatopek (1969) is “looking W-NW” but the true one is towards the S-SW.

(b) View of the scarp depicted in (a) in September, 2004 (looking S-SW). The view is closer to the W part of the scarp and more oblique to it, compared to (a). Dashed line and arrows indicate geomorphic features that permit correlation of the site to that depicted in (a). Differences in the valley side profile in the background are due to different angle of view.
(c) The western termination of the scarp in (a) and (b), across which the trench was excavated.

Figure 6. (a) Generalized stratigraphic features of the trench. Capital letters indicate litho-stratigraphic unit groups (channel fills), alphabetically from younger to older. FZ1 to 3 are fault zones. FZ1 and FZ3 have been active recently, affecting the upper part of the stratigraphy, whereas FZ2 is sealed. A subtle pressure ridge (push-up) is superposed on the fault scarp that coincides with FZ1 (along which the main 1967 rupture occurred). The ridge is bound to the S by FZ3.

(b) The perfectly parallel trend of channel A with respect to FZ1, as indicated by lines parallel to the fault zone, connecting the same features of the channel cross-profile on the two trench walls. This parallelism suggests that the channel was in all probability established here after the formation of a N-facing scarp by FZ1. The same relationship is observed between the N margin of channel H and FZ2.

Figure 7. (a, b) Logs of the eastern and western (reversed) trench walls. (c,d) Details of the logs of fault zones 1-3 on the eastern wall. Descriptions of stratigraphic units are given in Table 1. Only gravel clasts above a certain size are depicted in each unit, only to give a rough indication of the coarseness of various units (they do not depict bedding – compare with Figs. 8-11).

Figure 8. The event horizon of paleoearthquake I (FZ1-1), at the northern side of FZ1 (East wall). A triangular slice of laminated sands and two intervening gravel layers has been pushed up towards the North and warped in-between two fault strands, resulting in much steeper dips of the main bedding surfaces in the sands. The deformed slice is truncated by the non-deformed erosional bottom of a gravel layer A2.

Figure 9. Photomosaic and log of fault zone 2 and surrounding stratigraphy. Legend as in Figure 7. small arrows at the base of unit F1 indicate filling of burrows inside unit H1. Larger Arrow with question mark in units 200/200a indicates a probable similar case.

Figure 10. Photomosaic of fault zone 3 and surrounding stratigraphy. Legend as in Figure 7.

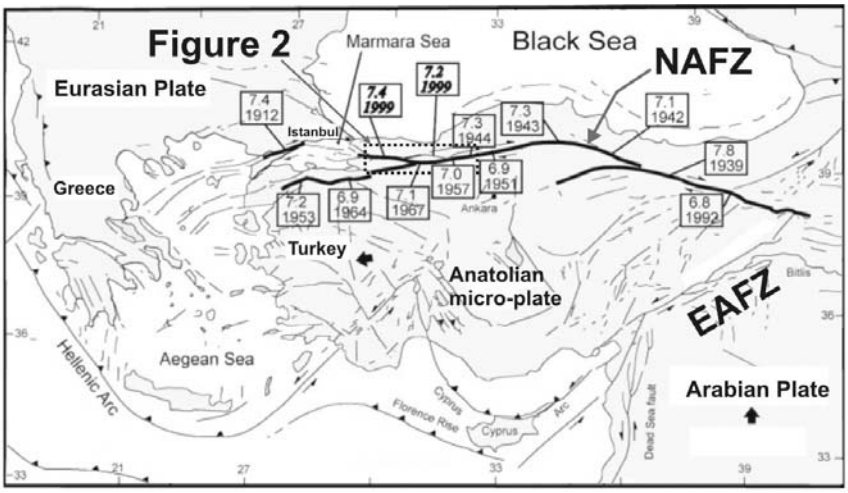
Figure 2
Marmara Sea
Black Sea
NAFZ
Eurasian Plate
7.4 1912
7.4 1999
7.2 1999
7.3 1944
7.3 1943
7.1 1942
7.8 1939
Istanbul
Greece
7.0 1957
6.9 1951
7.2 1953
6.9 1964
7.1 1967
6.8 1992
Ankara
Turkey
Anatolian micro-plate
EAFZ
Bitlis
Aegean Sea
Hellenic Arc
Arabian Plate
Cyprus
Florence Rise
Cyprus
Arc
Dead Sea fault

Fig. 1

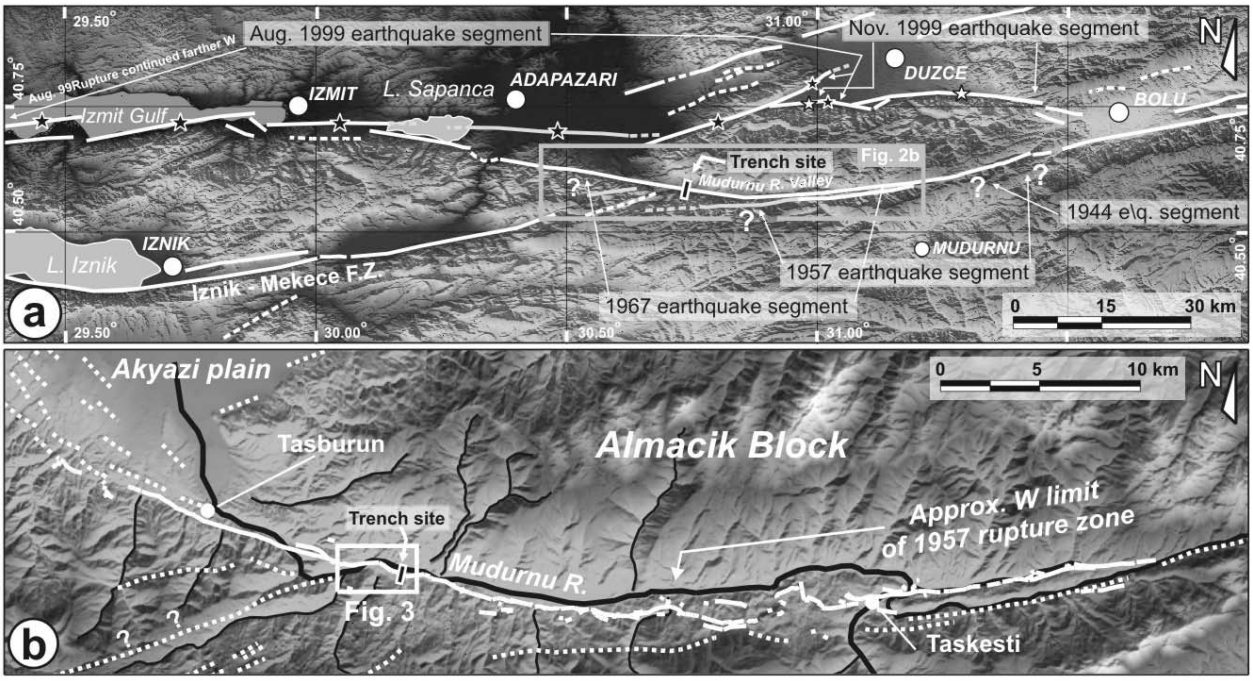
Aug. 1999 earthquake segment
Nov. 1999 earthquake segment
Aug. 99Rupture continued farther W
IZMIT
L. Sapanca
ADAPAZARI
DUZCE
BOLU
Izmit Gulf
Trench site
Fig. 2b
Mudurnu R. Valley
1944 e\q. segment
IZNIK
L. Iznik
MUDURNU
Iznik - Mekece F.Z.
1957 earthquake segment
1967 earthquake segment
0 15 30 km
a
Akyazi plain
0 5 10 km
Tasburun
Almacik Block
Trench site
Approx. W limit of 1957 rupture zone
Mudurnu R.
Fig. 3
Taskesti
b

Fig. 2

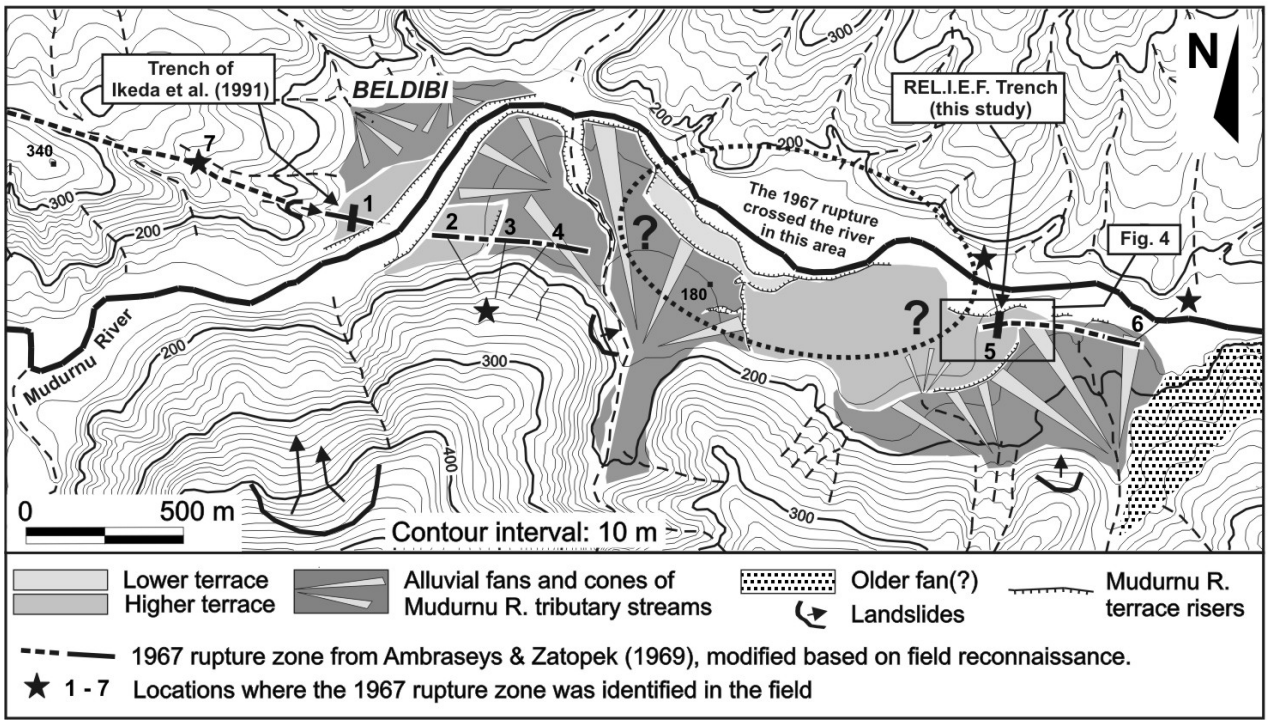
Trench of Ikeda et al. (1991)
BELDIBI
REL.I.E.F. Trench (this study)
N
The 1967 rupture crossed the river in this area
Fig. 4
Mudurnu River
0 500 m
Contour interval: 10 m
Lower terrace
Higher terrace
Alluvial fans and cones of Mudurnu R. tributary streams
Older fan(?)
Landslides
Mudurnu R. terrace risers
1967 rupture zone from Ambraseys & Zatopek (1969), modified based on field reconnaissance.
1 - 7 Locations where the 1967 rupture zone was identified in the field

Fig. 3

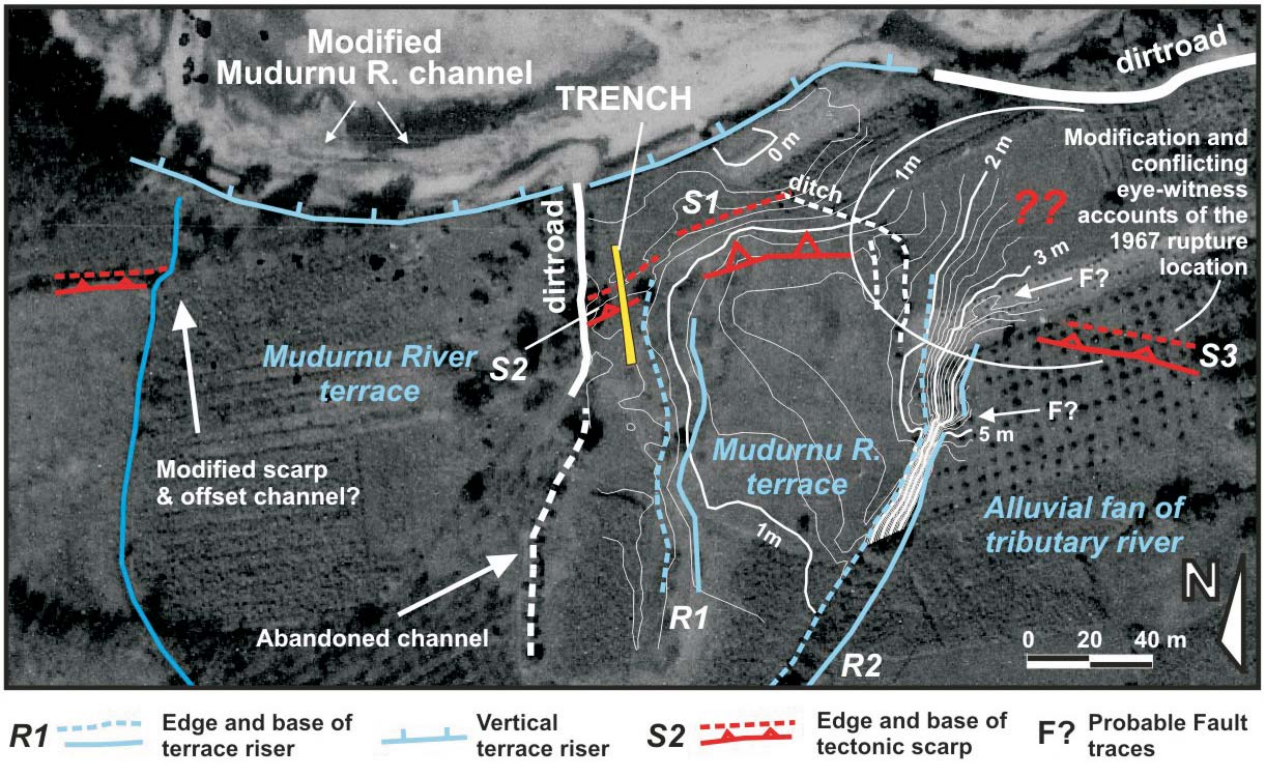
Modified Mudurnu R. channel
TRENCH
dirtroad
ditch
S1
S2
S3
Modification and conflicting eye-witness accounts of the 1967 rupture location
Mudurnu River terrace
Mudurnu R. terrace
Alluvial fan of tributary river
Modified scarp & offset channel?
Abandoned channel
R1
R2
N
0 20 40 m
R1 Edge and base of terrace riser
Vertical terrace riser
S2 Edge and base of tectonic scarp
F? Probable Fault traces

Fig. 4

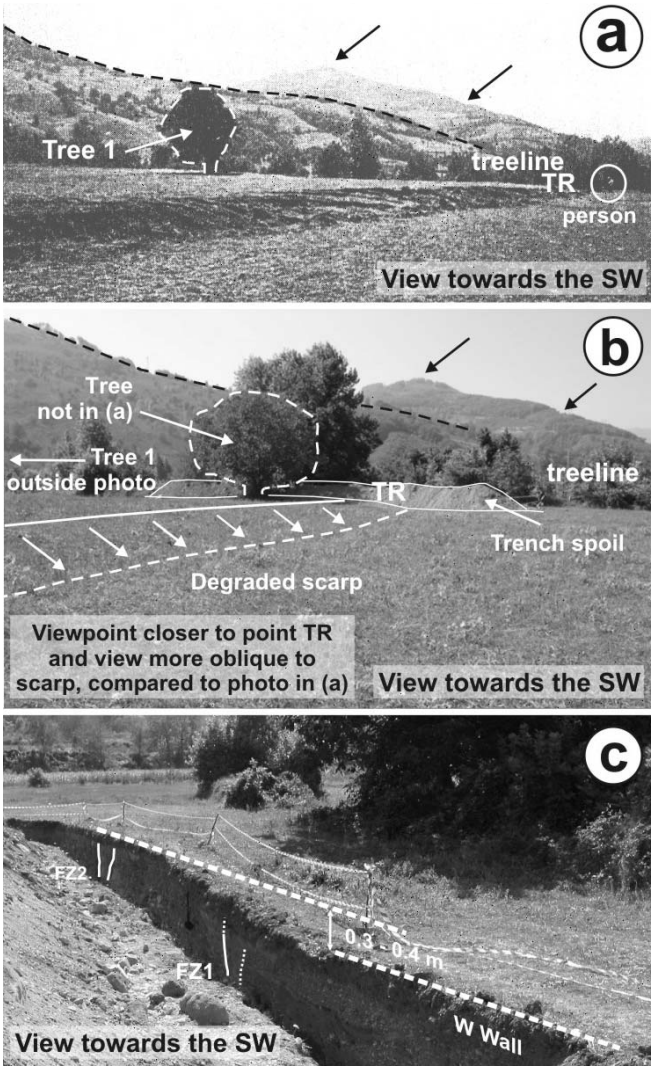

Fig. 5 B&W

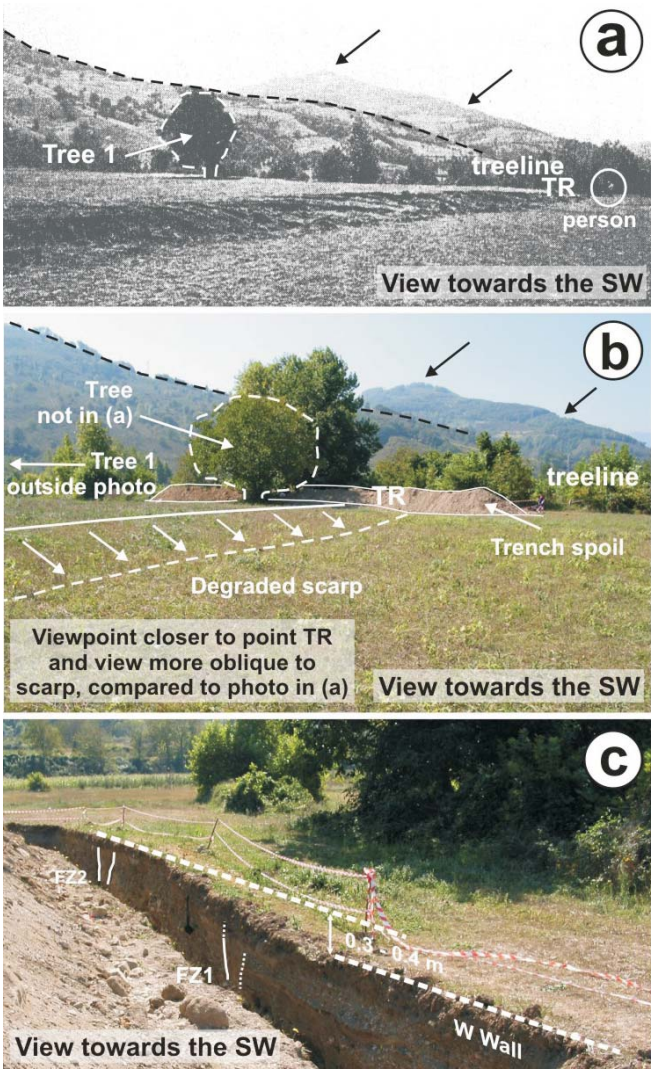

Fig. 5 Color

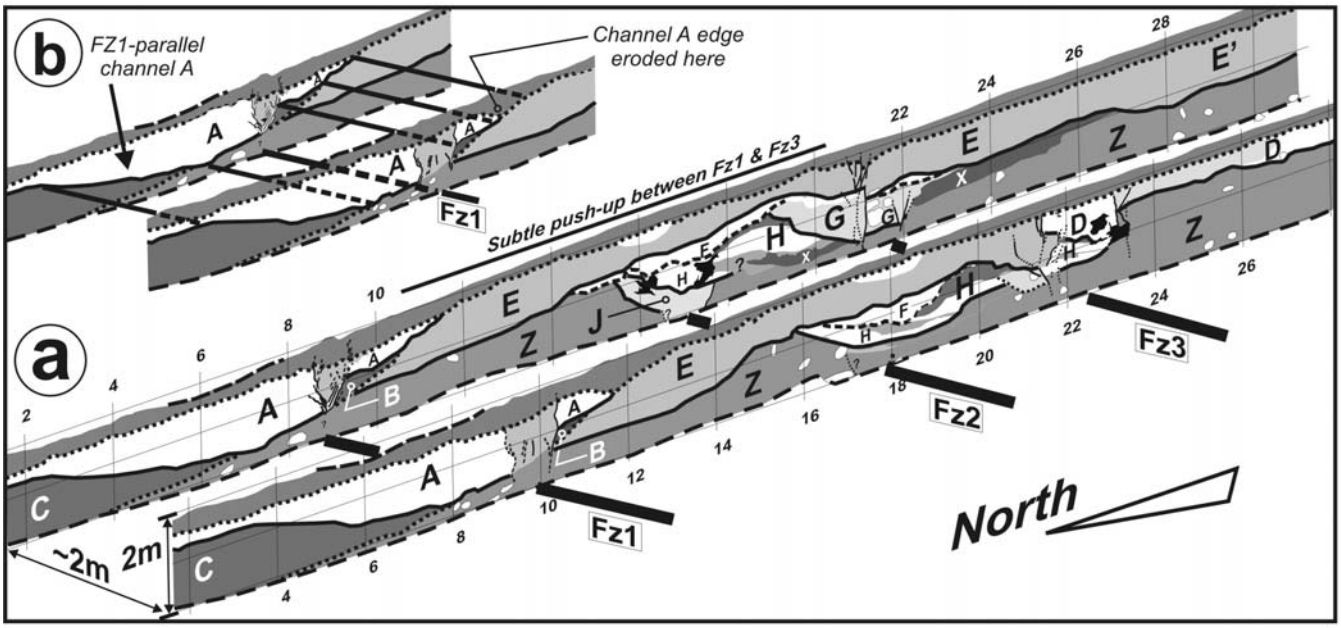

Fig. 6

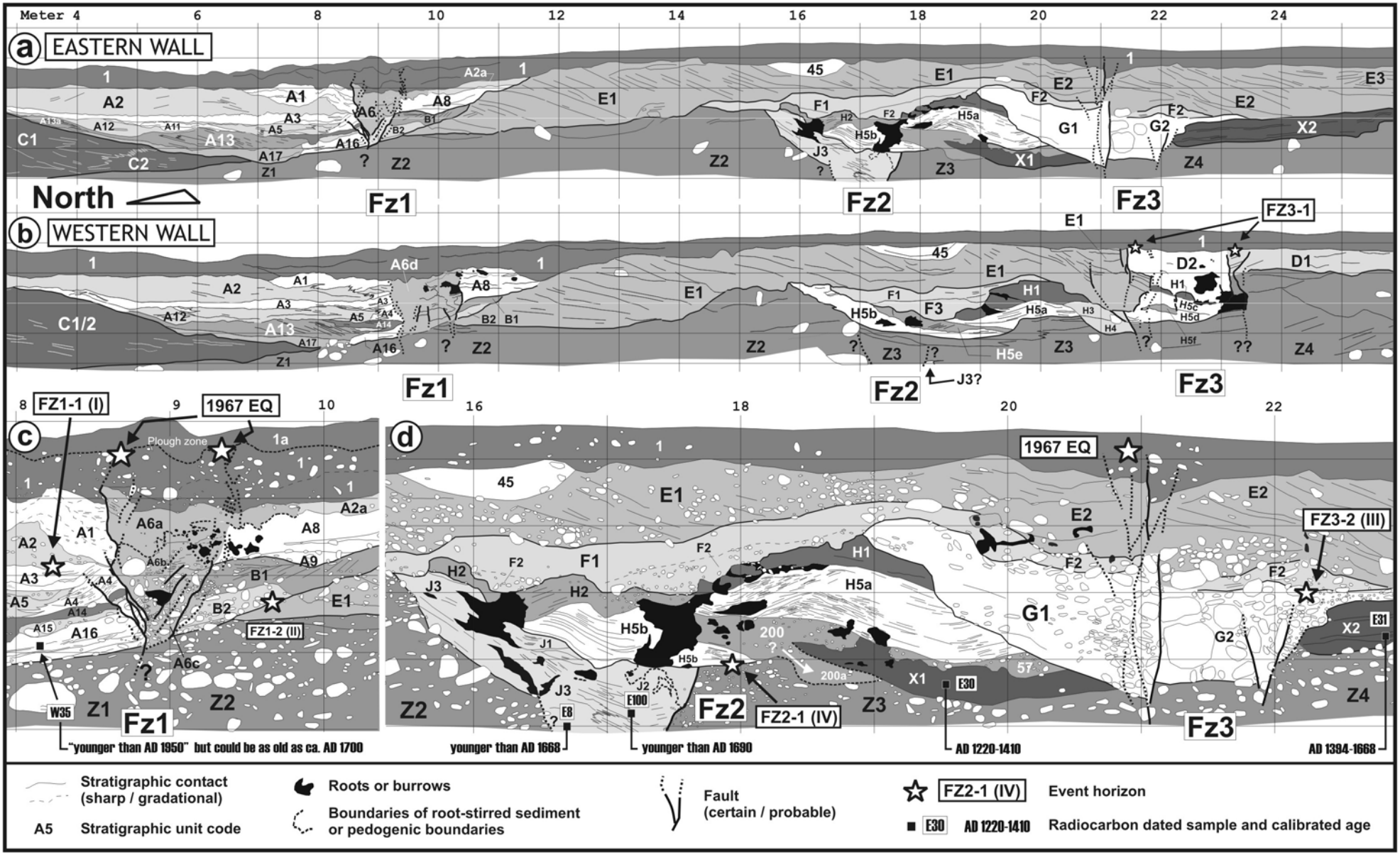
Meter 4 6 8 10 12 14 16 18 20 22 24
a EASTERN WALL
North
Fz1
Fz2
Fz3
b WESTERN WALL
FZ3-1
J3?
c
FZ1-1 (I)
1967 EQ
Plough zone
FZ1-2 (II)
W35
"younger than AD 1950" but could be as old as ca. AD 1700
d
1967 EQ
FZ3-2 (III)
FZ2-1 (IV)
E100
E8
E30
E31
younger than AD 1668
younger than AD 1690
AD 1220-1410
AD 1394-1668
Stratigraphic contact (sharp / gradational)
A5 Stratigraphic unit code
Roots or burrows
Boundaries of root-stirred sediment or pedogenic boundaries
Fault (certain / probable)
FZ2-1 (IV) Event horizon
E30 AD 1220-1410 Radiocarbon dated sample and calibrated age

Fig. 7

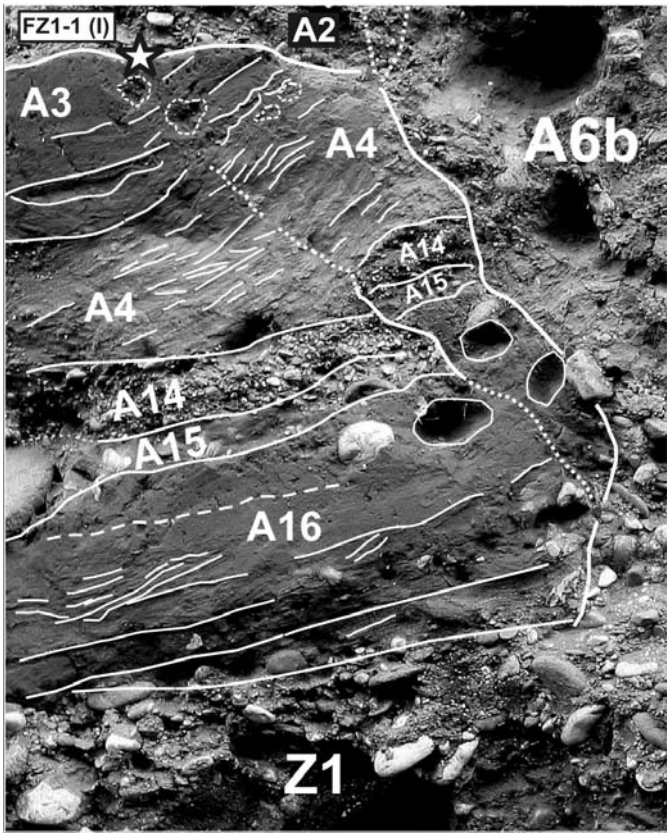

Fig. 8 B&W

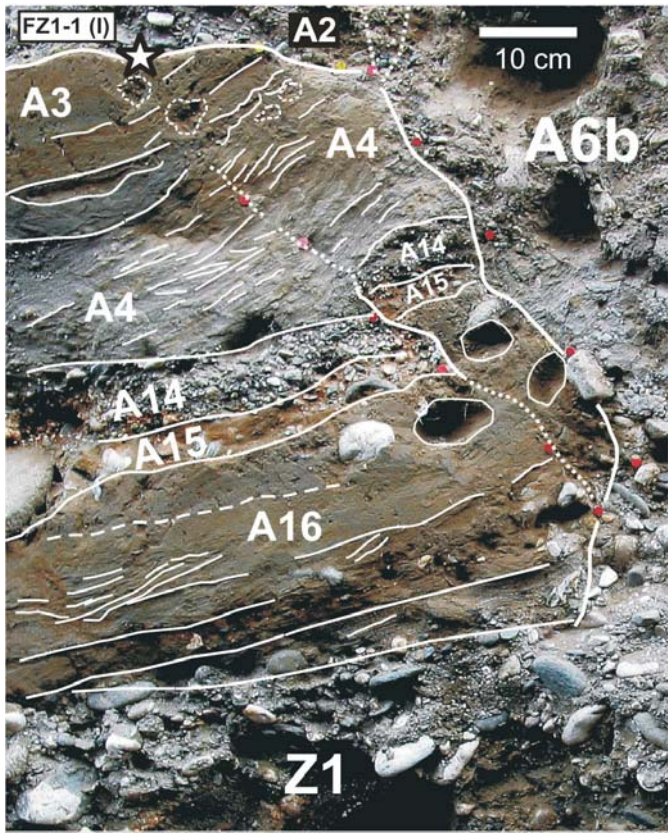

Fig. 8 Color

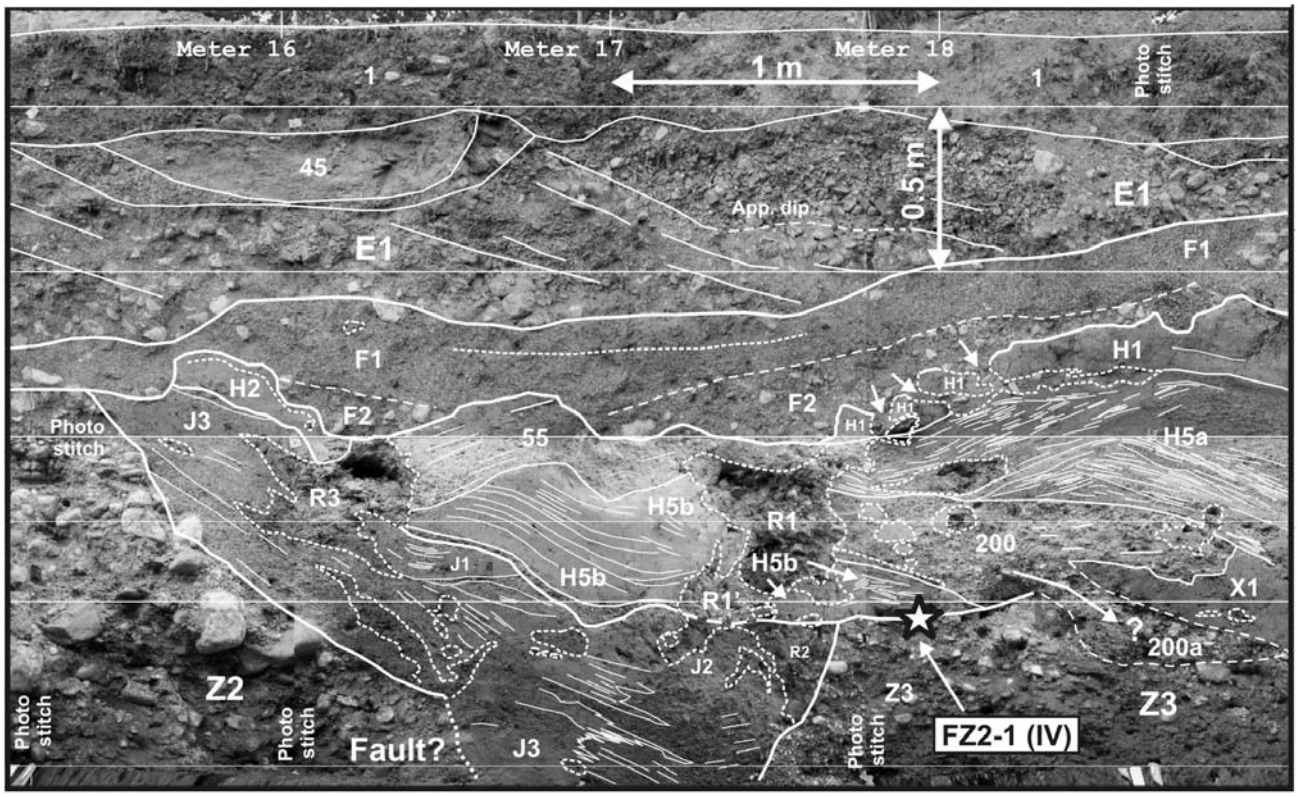

Fig. 9 B&W

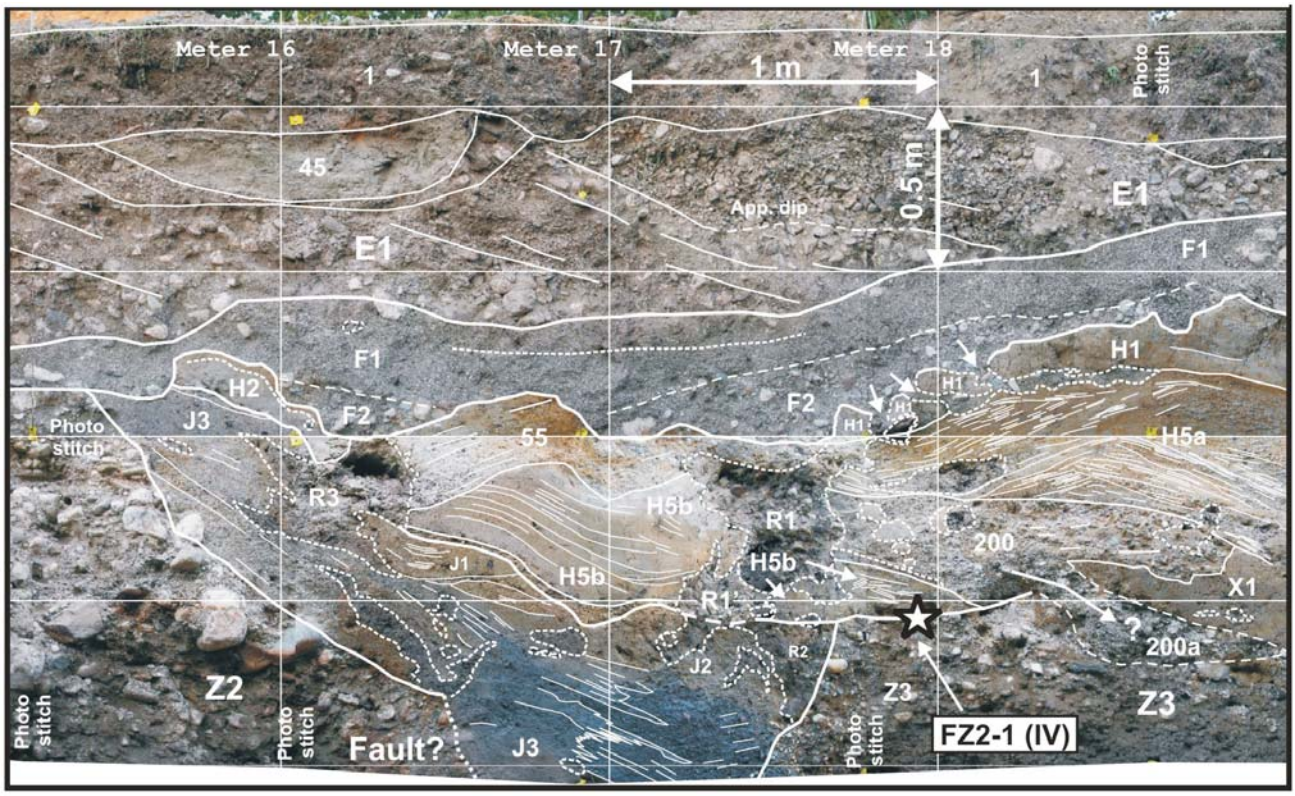

Fig. 9 Color

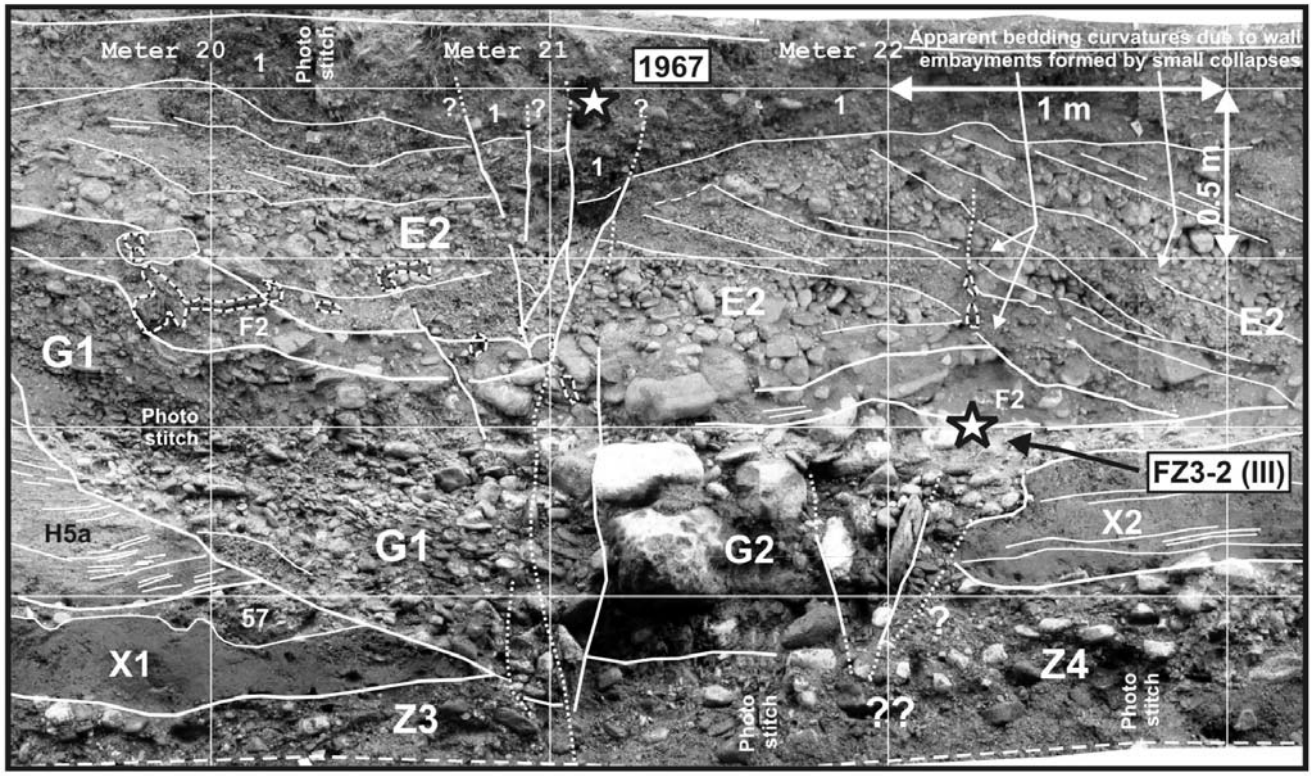

Fig. 10 B&W

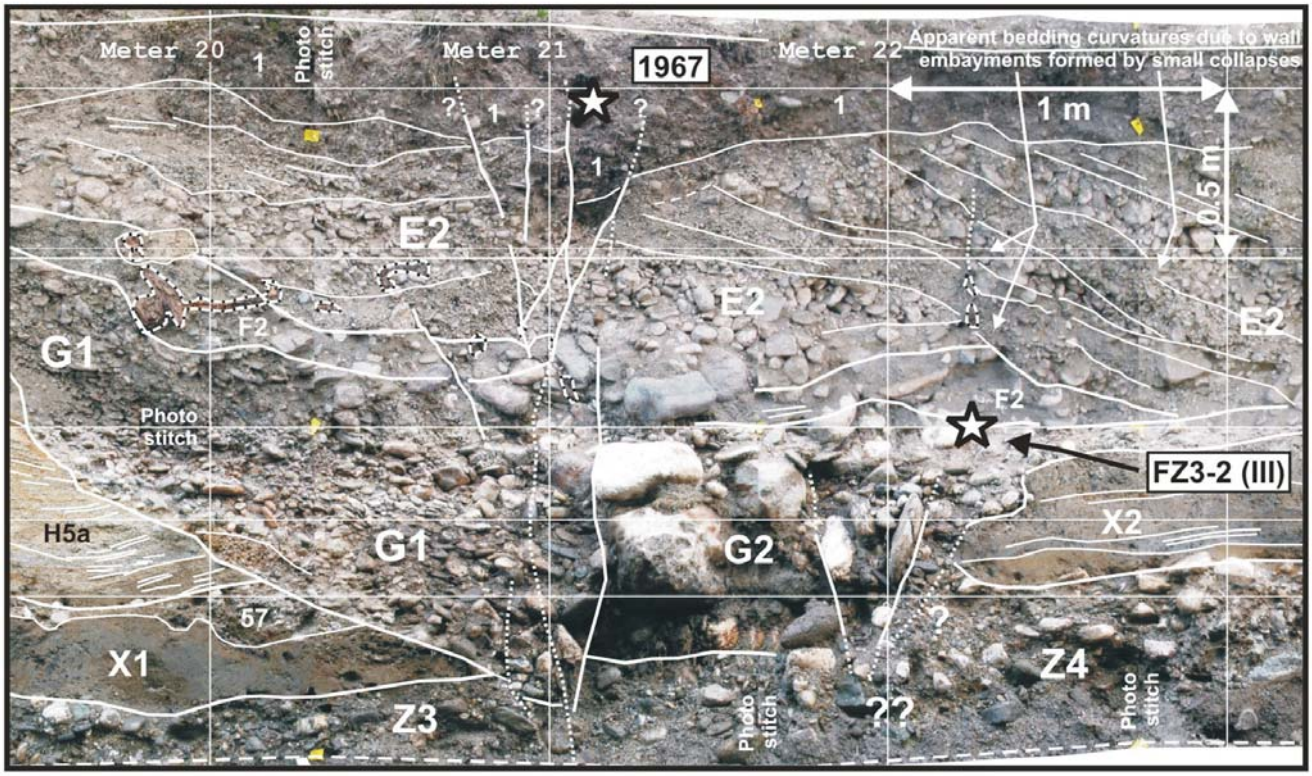

Fig. 10 Color